OFFICE OF NAVAL RESEARCH

Photogenerated Base in Polymer Curing and Imaging:The use of a-Keto Carbamates as Novel Photoprecursors of Amines

Jean M.J. Fréchet, James F. Cameron, and C. Grant Willson

Department of Chemistry, Baker Laboratory Cornell University
Ithaca, New York 14853-1301
and
IBM Research Division, Almaden Research Center
650 Harry Road, San Jose, California 95120-6099

June 1, 1995

DTIC QUALITY INSPECTED 3

19950605 030

REPORT DOCUMENTATION PAGE			Form Approved OMB No. 0704-0188

Public reporting burden for this collection of information is estimated to average 1 hour per response, including the time for reviewing instructions, searching existing data sources, gathering and maintaining the data needed, and completing and reviewing the collection of information. Send comments regarding this burden estimate or any other aspect of this collection of information, including suggestions for reducing this burden, to Washington Headquarters Services, Directorate for Information Operations and Reports, 1215 Jefferson Davis Highway, Suite 1204, Arlington, VA 22202-4302, and to the Office of Management and Budget, Paperwork Reduction Project (0704-0188), Washington, DC 20503.

1. AGENCY USE ONLY (Leave blank)	2. REPORT DATE	3. REPORT TYPE AND DATES COVERED Technical Report # 23	
4. TITLE AND SUBTITLE Photogenerated Base in Polymer Curing and Imaging:The use of a-Keto Carbamates as Novel Photoprecursors of Amines			**5. FUNDING NUMBERS** C N00014-91-1338
6. AUTHOR(S) Jean M.J. Fréchet, James F. Cameron, and C. Grant Willson			
7. PERFORMING ORGANIZATION NAME(S) AND ADDRESS(ES) Cornell University Dept. of Chemistry, Baker Laboratory Ithaca, New York 14853-1301			**8. PERFORMING ORGANIZATION REPORT NUMBER** C N00014-91-1338
9. SPONSORING/MONITORING AGENCY NAME(S) AND ADDRESS(ES) Department of the Navy Office of Naval Research 800 North Quincy Street Arlington, VA 22217-5000			**10. SPONSORING/MONITORING AGENCY REPORT NUMBER**

11. SUPPLEMENTARY NOTES

12a. DISTRIBUTION/AVAILABILITY STATEMENT Reproduction in whole or in part is permitted for any purpose of the United States Government. This document has been approved for public release and sale, its distribution is unlimited.	**12b. DISTRIBUTION CODE**

13. ABSTRACT (Maximum 200 words)

Several newly developed a-keto carbamates are useful as photoprecursors of amines. These photogenerated catalysts that are designed primarily for use in chemically amplified resist materials can also be used for the curing of polymers containing base crosslinkable reactive groups. The new a-keto carbamates can undergo light triggered photocleavage both in the solid-state and in solution to give free amines. The photoactive benzoinyloxycarbonyl groups of these compounds are active with ultraviolet radiation below 400nm. The influence of various steric and electronic effects on the photoliberation of free amines from a-keto carbamates has been studied and the effect of structural modification of the aryl rings was used to probe the electronic factors of the photocyclization. The great potential of these photoactive carbamates as organic sources of photogenerated amines was demonstrated using both classical spectroscopic techniques (UV, IR and NMR) and GC-MS analysis of the photolysis products. In all cases the photocleavage reaction is near quantitative and the quantum yields have been measured over a range of wavelengths from 250-370 nm.

14. SUBJECT TERMS Photopolymer, curing, imaging, photogenerated base microlithography, display technology, amine precursor photogenerated catalyst, photochemistry			**15. NUMBER OF PAGES** 42
			16. PRICE CODE
17. SECURITY CLASSIFICATION OF REPORT Unclassified	**18. SECURITY CLASSIFICATION OF THIS PAGE** Unclassified	**19. SECURITY CLASSIFICATION OF ABSTRACT** Unclassified	**20. LIMITATION OF ABSTRACT** UL

NSN 7540-01-280-5500

Standard Form 298 (Rev. 2-89)
Prescribed by ANSI Std. 239-18
298-102

Photogenerated Base in Polymer Curing and Imaging:
The use of α-Keto Carbamates as Novel Photoprecursors of Amines

Jean M.J. Fréchet, James F. Cameron, and C. Grant Willson

Department of Chemistry, Baker Laboratory, Cornell University

Ithaca, New York 14853-1301

and

IBM Research Division, Almaden Research Center

650 Harry Road, San Jose, California 95120-6099

Summary.

Several newly developed α-keto carbamates are useful as photoprecursors of amines. These photogenerated catalysts that are designed primarily for use in chemically amplified resist materials can also be used for the curing of polymers containing base crosslinkable reactive groups. The new α-keto carbamates can undergo light triggered photocleavage both in the solid-state and in solution to give free amines. The photoactive benzoinyloxycarbonyl groups of these compounds are active with ultraviolet radiation below 400nm. The influence of various steric and electronic effects on the photoliberation of free amines from α-keto carbamates has been studied and. the effect of structural modification of the aryl rings was used to probe the electronic factors of the photocyclization. The great potential of these photoactive carbamates as organic sources of photogenerated amines was demonstrated using both classical spectroscopic techniques (UV, IR and NMR) and GC-MS analysis of the photolysis products. In all cases the photocleavage reaction is near quantitative and the quantum yields have been measured over a range of wavelengths from 250-370 nm.

1

Introduction.

While early studies with photochemically labile protecting groups have originally been carried out with the goal of simplifying complex synthetic schemes,[1] their use has more recently been extended to a variety of application in microlithography.[2-4] A number of photodeprotection schemes that also require the controlled release of reactive species *in-situ* include caged biomolecule release,[5] or combinatorial solid phase peptide synthesis.[6]

Our original work[3] with chemically amplified resist materials has involved the in situ phototriggered formation of acid within a reactive polymer film. The now well known family of resists[2] based on the chemistry of polymers with t-butyl carbonate (t-BOC) and t-butyl ester groups has been used commercially by IBM for the mass production[4] of DRAM memory chips since the early 1980's. Numerous others have used our approach in the design of analogous resist materials that also involve the photogeneration of acid in the key imaging step.[7] In contrast, the complementary approach of base photogeneration has received little attention[8]. Recently, we have developed a strategy for base photogeneration by masking amines and diamines as photoactive carbamates[9,10]. Under the action of light, these reactive carbamates decompose to liberate the base in a reactive form. The first generation of photoprecursors of organic base are already finding application in a variety of imaging schemes requiring photogenerated base[11]. The success of our amine photorelease strategy is further illustrated by the development of a number of base catalyzed chemically amplified resist materials[12-13].

Of all the common photolabile amino protecting groups, we found that those derived from the 3,5-dimethoxy-α,α-dimethylbenzyloxycarbonyl (Ddz) and *o*-nitrobenzyloxycarbonyl moieties[9] are particularly well suited to the photogeneration of organic base. While base photogenerators derived from these photoprotecting groups have proven useful, they do suffer from some restrictions . For instance, the utility of the *o*-nitrobenzyl class of base photogenerator is limited by the formation of reactive *o*-nitrosocarbonyl compounds, which may be toxic and also may undergo deleterious side reactions[9] . Over-irradiation products such as azo-coupled intermediates act as internal light filters and ultimately restrict the use of these base photogenerators to thin film applications[11-13]. Similarly, severe anti-bleaching is a significant problem with the 3,5-dimethoxy-α,α-dimethylbenzyloxycarbonyl class of photobase generators[9].

It is these potential limitations of our first generation of amine photoprecursors that has prompted the development of new photochemistry for organic solid state applications. As indicated in the previous report, desyl photochemistry offers several desirable features which render it particularly attractive for base photogeneration. These features include improved photoefficiency, enhanced rate of photorelease and increased stability of the photo by-products. In this report, we describe novel applications of benzoin photochemistry to the preparation of efficient photoprecursors of organic bases: primary and secondary amines. Encouraged by preliminary results from the solution photolysis of cyclohexylamino and piperidino carbamates of 3',5'-dimethoxybenzoin[14], we focus further on the novel photorearrangement of the 3',5'-dimethoxybenzoin chromophore (Scheme 1). while the preceding report described the synthesis of a variety of carbamates based on the 3',5'-dimethoxybenzoin chromophore and its substituted analogs, we now focus on the photochemistry of a these α-keto carbamates. The carbamates were chosen for detailed evaluation based on 1) their synthetic accessibilty and 2) their ability to contribute to structure-activity relationships pertinent to base photogeneration. Our aim is to provide a basic understanding of the issues that determine the efficiency of amine photogeneration from 3',5'-dimethoxybenzoin carbamates and substituted derivatives.

Results and Discussion.

1) Design Considerations

Previous experience in designing base photogenerators[9], suggests some of the most critical features to consider include: 1) favorable UV characteristics, 2) quantum efficient photodecomposition, 3) solid-state photoreactivity, 4) photorelease of the base in a reactive form, 5) stability of photo by-products 6) thermal stability, 7) ease of synthesis. This list is only a general guide because specific applications place additional custom requirements on any base photogenerator. The materials chosen for detailed study were restricted to the cyclohexylamine photogenerators shown in Scheme 2. By only selecting photoprecursors of cyclohexylamine, a direct comparison of the chromophore structure-photosensitivity relationship could be readily made. The α-keto carbamates of interest are those containing the following chromophores; the parent desyl group as in **(1)**, the 3,3',5,5'-tetramethoxybenzoin moiety as in **(2)**, the 3,5-dimethoxybenzoin group as in **(3)**, the 3',4,5'-trimethoxybenzoin moiety as in **(4)**, the 3',5-dimethoxy-4-methylthiobenzoin group as in **(5)**, 2-(3,5-

3

dimethoxyphenyl)-1-(2-naphthalenyl)ethanone as in (6) and 2,2-di-(3',5'-dimethoxyphenyl)-1-phenylethanone as in (7). These materials are characterized in terms of the design criteria outlined above.

2) Photochemistry of Carbamates Derived from α-Hydroxy Ketones

α-Keto carbamates absorb UV light from just below 370 nm down to the deep UV. Excitation of the carbonyl chromophore is believed to cause photocyclization to the benzo[b]furan with concomitant liberation of the amine type base (Scheme 1 and 2). Due to the nature of the α-keto chromophore, UV exposure at longer wavelengths is thought to cause photocyclization via direct n-π* excitation. However, photolysis at the higher energy end (π-π* excitation) can also result in the liberation of base although the photocyclization may proceed less efficiently as it requires some energy transfer process. A variety of the spectroscopic methods e.g. ^{1}H NMR, IR, and UV proved useful in monitoring the photochemistry of these new photogenerators. GC and GC-MS facilitated identification of the photoproducts.

a) Solution Photosensitivity

i) Photochemistry of Unsubstituted α-Keto Carbamates

Monitoring the photolysis of benzoin cyclohexyl carbamate (1) by a number spectroscopic methods served to indicate the complexity of the photochemistry of the α-keto chromophore. A significant conversion of benzoin cyclohexyl carbamate (1) to free cyclohexylamine was observed on monitoring the photolysis by ^{1}H NMR spectroscopy (Table 1). However, despite the high conversion, no evidence was observed for the clean photocyclization. In fact, the ^{1}H NMR spectrum became very complicated, implying that photodecomposition of this material proceeds by a variety of competing pathways. This was further confirmed by monitoring the photolysis of benzoin carbamate (1) by infra-red spectroscopy. In this case, the keto carbonyl stretch (1699 cm^{-1}) disappears while the carbamate carbonyl stretch (1722 cm^{-1}) remains substantially intact. A weak carbonyl stretch at 1658 cm^{-1} also appears possibly due to photooxidation. These observations are consistent with photodecomposition of benzoin carbamate (1) proceeding by a variety of mechanisms of which photocyclization to benzo[b]furan

plays only a minor role. Furthermore, a complex multicomponent mixture is observed by TLC after 350 nm photolysis of benzoin carbamate (**1**).

ii) Photochemistry of Aryl substituted α-Keto Carbamates

The importance of the meta activation by 3',5'-dimethoxy substituents in the photocyclization of α-keto carbamates to benzo[b]furans is apparent in the 350 nm solution photolysis of some α-keto carbamates as readily monitored by ^{1}H NMR spectroscopy in dry, degassed acetonitrile-d3. Table 1 shows examples of α-keto carbamates which undergo efficient photogeneration of cyclohexylamine on 350 nm photolysis. For all these carbamates, the integral of the carbamate cyclohexyl methine [cyclohexyl CH, m, δ ~ 3.2-3.4 (dependent on exact structure of photosensitive carbamate)] decreased, while the expected multiplet of the cyclohexyl methine of free cyclohexylamine appeared at δ 2.52, with increasing 350 nm exposure in a Rayonet photochemical reactor. By ratioing the cyclohexyl methine integral for free cyclohexylamine to the aryl resonances, the % conversion after 60 min. 350 nm exposure was calculated for a variety of α-keto carbamates as shown in Table 1. % Conversion varied from 37-98% depending on the chromophore structure. Besides identifying cyclohexylamine, ^{1}H NMR spectroscopy allowed the expected benzo[b]furan to be identified as the major photo by-product on 350 nm photolysis of 3',5'-dimethoxy substituted benzoin carbamates, (**2**), (**3**), (**4**), (**5**) and (**6**). A characteristic singlet of the 3-benzo[b]furan proton in the photoproduct mixture appears with increasing photolysis. The chemical shift of this proton is included in Table 1. In these systems which undergo smooth photocyclization, the % conversion for formation of benzo[b]furan tends to parallel that for amine generation. The cleanliness of the photocyclization of these 3,5-dimethoxy activated benzoin carbamates is nicely illustrated by following the changes in the ^{1}H NMR aryl resonances with increasing exposure dose for the conversion of carbamate (**2**) to benzo[b]furan (**2a**) in tetrahydrofuran-d8 (Figure 1). A plot of % conversion against irradiation time for the 350 nm photolysis of carbamate (**2**) further demonstrates the efficiency of the benzoin photocyclization (Figure 2). The same clean photochemistry is not apparent with other α-keto carbamates. For instance, systems lacking the 3',5'-dimethoxy substitution pattern e.g., (**1**) undergo particularly complex photodecomposition.

5

The clean photogeneration of free cyclohexylamine from all 3',5'-dimethoxy substituted benzoin carbamates was further confirmed by both gas chromatography using coinjection and GC-MS studies ($C_6H_{11}NH_2$ $M^+=99$). For these cyclohexyl carbamates, (2), (3), (4), (5) and (6), GC-MS indicated the major by-products were the expected substituted benzo[b]furans (2a), (3a), (4a), (2a) and (6a) respectively. Other minor products were identified as the corresponding benzylic ketone e.g. (2b), the corresponding substituted benzil e.g. (2c), the corresponding N-acylcyclohexylamine e.g. (2d) and dicyclohexylurea (Scheme 2). Formation of these minor photoproducts can be rationalized in terms of the known benzoin photochemistry. For instance, the benzylic ketone e.g. (2b), is formed by loss of the carbamoyloxy moiety. This mode of photocleavage is common in benzoin photochemistry and tends to occur when a good leaving group is present at the α-keto position. Indeed, the photolabile phenacyl protecting group is known to cleave via this pathway[15]. The benzil photoproduct e.g. (2c), is likely formed by cleavage of the oxycarbonyl bond followed by photooxidation. In the case of unsymmetrical benzoin carbamates, only the corresponding unsymmetrical benzil was identified by GC-MS. Since there was no indication of any symmetrical benzils, formation of these 1,2-ethanediones is unlikely to be the product of acyl radical recombination. Similar cleavage of oxycarbonyl bonds is known to occur in appropriately substituted benzoins. For instance, photolysis of 4,4'-dimethoxybenzoin acetate is known to from 4,4'-dimethoxybenzil as the major product[16]. As for the N-acylcyclohexylamine e.g. (2d), this class of photoproduct is likely formed by combination of acyl and cyclohexylamino radicals. The acyl radicals are most likely formed by the well known Norrish Type I photocleavage. Cyclohexylamino radicals may be formed in a number of ways. For example, the carbamoyloxy radicals liberated in the formation of the benzylic ketone e.g. (2b), will likely undergo facile decarboxylation. Alternatively, cleavage of the oxycarbonyl bond to give the substituted benzil e.g. (2c), would be accompanied by formation of a N-formylcyclohexylamino radical. This species would be expected to liberate cyclohexylamino radicals via decarbonylation. Interestingly, no indication of the corresponding aldehyde from the acyl radical formed by Norrish Type 1 cleavage was available by GC-MS. This implies recombination of acyl and amino radicals is strongly favored over hydrogen abstraction. The presence of trace amounts of dicyclohexylurea can be rationalized as follows. Combination of N-formylcyclohexylamino and cyclohexylamino radicals would give dicyclohexylurea. Another possibility is

6

the reaction of photogenerated cyclohexylamine with cyclohexyl isocyanate. The isocyanate being formed by loss of a hydrogen atom from the N-formylcyclohexylamino radical.

Further evidence for the photochemical rearrangement of these α-keto carbamates was obtained by following the changes in the infra-red spectrum of a solution of carbamate (3) in dry acetonitrile with increasing UV exposure dose. As seen in Figure 3, 350 nm Rayonet exposure of carbamate (3) caused the gradual disappearance both the keto carbonyl stretch (1700 cm^{-1}) and the carbamate carbonyl stretch (1723 cm^{-1}). This change is consistent with the proposed mode of photodecomposition (Scheme 2) in which photocyclization to liberate the free amine causes these stretches to disappear . In addition, evidence for the photogeneration of free amine was gained by monitoring the changes in the N-H stretching frequency of this substrate (3) (Figure 4). In this case, UV exposure at 350 nm resulted in the gradual depletion of the carbamate N-H stretch at 3360 cm^{-1}, with concomitant appearance of stretches due to the photogenerated cyclohexylamine in the region 3500 to 3700 cm^{-1}. Similarly smooth disappearance of both carbonyl stretches was observed on irradiation of carbamates (2) and (4). These findings are consistent with smooth photocyclization and concomitant amine liberation occurring in these 3',5'-dimethoxy substituted benzoin carbamates. In the case of carbamates, (5) and (6), the disappearance of both carbonyl groups was complicated by the appearance of two weak absorptions at 1675 and 1685 cm^{-1} respectively. This indicates the photocyclization of carbamates (5) and (6) is complicated by alternate side reactions open to the desyl chromophore. These include photocleavage by Norrish Type I and C-O homolytic pathways, both of which would produce carbonyl containing products. Such competing photochemistry may also explain the slightly lower yields for amine generation from carbamates (5) and (6) (Table 1).

Beyond 350 nm, the extinction coefficients of these carbamates is typically of the order 50-200 L mol^{-1}·cm^{-1}. Considering the low absorption of these carbamates at longer wavelengths, the efficiency of the photocyclization and concomitant amine generation on 350 nm photolysis is truly remarkable. In addition carbamates which absorb the most light at longer wavelengths are not the most efficient according to ^{1}H NMR studies. For instance, amine photogeneration from carbamate (6) ($\varepsilon_{(365)}$ 212 L mol^{-1}·cm^{-1}) is less efficient than carbamate (2) ($\varepsilon_{(365)}$ 45 L mol^{-1}·cm^{-1}). This indicates a subtle relationship exists between photocyclization and the nature of the benzoyl chromophore.

7

In carbamates containing bathochromic substituents, the UV spectrum of these materials was strongly influenced out to ca. 340 nm. For example, the 4-thiomethyl substituted carbamate (5) and the 1-naphthalenyl carbamate (6) had extinction coefficients at 336 nm of 5049 and 2008 L mol^{-1} cm^{-1} respectively. Therefore, it is apparent that structural variation of the benzoyl chromophore does influence the long wavelength absorption. However, in these systems the absorption drops off quickly beyond 340 nm and the substituent effect is not strong enough to cause a significant bathochromic shift out to 350 nm.

The result of following the changes in the UV spectrum of a dilute solution of carbamate (2) is shown in Figure 5. Three isobestic points are observed: 251, 266 and 340 nm respectively. Overall, the change in the UV spectrum is representative of this class of α-keto carbamates and is consistent with photocyclization to form the corresponding benzo[b]furan (2a) (Scheme 2). During irradiation of carbamate (2), the maxima originally at 267 nm is replaced by an intense absorption maxima at 300 nm. due to photocyclization to the conjugated benzo[b]furan (2a). Interestingly, the absorption due to the aryl π-π* transition (250-265 nm) decreases on photocyclization. Furthermore, beyond ca.340 nm, the absorption tail of the carbonyl chromophore disappears with increasing 350 nm photolysis. This bleaching of the long wavelength n-π* transition was only observed for 3,3',5,5'-tetramethoxybenzoin carbamate (2). Other derivatives e.g. (3) and (6) only show bleaching of the deep UV π-π* absorption while carbamates (4) and (5) show antibleaching. The propensity for bleaching of both the long wavelength tail (> 340 nm) and the deep UV absorption (ca. 250-265 nm) is a particularly attractive feature of this photogenerator (2). Based on the observed photobleaching of carbamate (2), this material holds particular promise as a photocatalyst in thick film applications at both deep UV and far UV exposure wavelengths. This is in contrast to the o-nitrobenzyl derived class of photobase generators in which anti-bleaching has restricted their use in some applications. The overlay plot (Figure 5) generated on solution photolysis of α-keto carbamates is comparable to that reported by Sheehan et. al.[17] for 3',5'-dimethoxybenzoin acetate. This is encouraging in that photocyclization to liberate amine seemingly proceeds by an analogous pathway to that used to liberate carboxylic acids (vide infra). The photolysis of 3',5'-dimethoxy substituted carbamates, (2) through (6), is remarkably clean by TLC. In these instances, the respective benzo[b]furans, (2a) through (6a) are the major products, and only trace amounts of other by-products are present.

8

<u>Preparative photolysis</u>

Preparative photolysis of cyclohexyl carbamates of both 3,3',5,5'-tetramethoxybenzoin (**2**) and 3',5'-dimethoxybenzoin (**3**) proceeded smoothly in acetonitrile. In both cases, the major products were cyclohexylamine and the appropriate substituted benzo[b]furan (**2a**) and (**3a**), respectively. The fluorescent benzo[b]furans were isolated as the major photoproducts in excellent yields (80-85%) by flash chromatography. In the case of 3,3',5,5'-tetramethoxybenzoin cyclohexyl carbamate (**2**), a deoxybenzoin photoproduct (**2b**), formed by loss of the carbamoyloxy moiety, was also isolated in 7% yield from the photolysate. Formation of such products have also been observed during GC-MS product studies (vide supra). Comparison of the extinction coefficients of the starting carbamates with the respective benzo[b]furan photoproducts indicates that the photoproducts absorb significantly less light in the 250-265 nm region. For example, the extinction coefficient of 3',5'-dimethoxybenzoin cyclohexyl carbamate (**3**) at 254 nm is 12341 L mol^{-1}·cm^{-1}, while that of 2-phenyl-5,7-dimethoxybenzofuran (**3a**) is 5972 L mol^{-1}·cm^{-1}. This difference explains the deep UV photobleaching of these photoactive carbamates.

iii) Photochemistry of 2,2'-Di-substituted α-Keto Carbamates

By ^{1}H NMR spectroscopy, the 2,2'-diaryl substituted cyclohexyl carbamate (**7**) was observed to photoliberate a significant amount of free cyclohexylamine (Table 1). However, no evidence for the formation of benzo[b]furan (**7a**) was available by ^{1}H NMR spectroscopy. By GC-MS, only cyclohexylamine, dicyclohexylurea and N-benzoylcyclohexylamine could be identified. Infra-red spectroscopy indicated that photocyclization proceeds somewhat sluggishly, with both the keto carbonyl stretch at 1700 cm^{-1} and the carbamate carbonyl stretch at 1727 cm^{-1} slowly disappearing on 350 nm Rayonet exposure. However, the rate of disappearance of the keto carbonyl stretch is faster than the carbamate carbonyl stretch and a weak absorption appears at 1685 cm^{-1}. Overall, photolytic studies on the 2,2'-disubstituted α-keto carbamate (**7**) resemble the less efficient 3',5'-dimethoxybenzoin carbamates (**5**) and (**6**). Based on these experimental observations, it seems likely that 2,2'-disubstituted α-keto carbamates undergo amine photogeneration via a number of competing pathways, in which photocyclization plays only a minor role.

b) Solid-State Photosensitivity

i) Photochemistry of Unsubstituted α-Keto Carbamates

Based on the results of monitoring the solution photochemistry of this class of benzoin derived base photogenerators, the solid state photodecomposition of these α-keto carbamates was investigated in limited detail. The solid state photodecomposition was conveniently monitored by irradiating thin poly(methacrylonitrile) (PMAN) films containing a few mol % benzoin carbamate (1) and following the changes in the UV spectrum. The change in the UV spectrum is inconsistent with efficient photocyclization to form the corresponding benzo[b]furan (1a) because the long wavelength n-π* transition of the carbonyl chromophore does not disappear. This observation is in agreement with the solution IR study, in which both carbonyl absorptions did not disappear during UV exposure. Although the mechanism of cyclohexylamine photogeneration may not proceed solely via photocyclization, benzoin cyclohexyl carbamate (1) has been reported to be an efficient base photogenerator for deep UV lithography[18]. This probably stems from the ability of benzoin cyclohexyl carbamate (1) to photoliberate cyclohexylamine via alternate pathways and in such applications is likely aided by the observed bleaching at 254 nm.

ii) Photochemistry of Aryl substituted α-Keto Carbamates

The intramolecular nature of the photocyclization of 3',5'-dimethoxy substituted benzoins suggests that photogeneration of amines can be effected in the solid state. This proved to be the case with all benzoin carbamates containing this substitution pattern undergoing photodecomposition as monitored by infrared and UV spectroscopy. The solid state photoreactivity was established by coating sodium chloride and quartz substrates with 1 μm thick poly(methylacrylonitrile) (PMAN) films containing approximately 5 mol % of the benzoin carbamate.

Photocyclization was monitored using infrared spectroscopy to follow the simultaneous disappearance of both keto and carbamate carbonyl absorptions with increasing UV exposure dose. Photocyclization to liberate base was found to be general in nature, and occurred on irradiation over a broad range of wavelengths ranging from deep UV to far UV. For instance, 3,3',5,5'-tetramethoxybenzoin carbamate (2) undergoes photocyclization to liberate cyclohexylamine on irradiation 254, 313, 336 and 365 nm. The observed change in the infrared spectrum on 254 nm photolysis of such films is illustrated for the photocyclization of α-keto carbamate (2) (Figure 6). There is a substantial difference in the extinction coefficients at 254 and 365 nm in these carbamates. For example, the extinction coefficient of carbamate (2) at 254 nm is 6180 L mol^{-1}·cm^{-1}, while at 365 nm it is 102 L mol^{-}

1 cm⁻¹. In a ca. 1 μm thick PMAN films containing 5 mol % of carbamate (2), this amounted to absorption of 78.8% of the light at 254 nm and only 7.1% of the light at 365 nm. However, despite the low absorption at 365 nm, the photochemistry is still relatively efficient at such long wavelengths.

The result of following the changes in the UV spectrum of thin films of PMAN containing about 5 mol % α-keto carbamate (3) on 254 nm exposure is shown in Figure 7. The deep UV maxima at 270 nm is replaced by an intense absorption maxima at 300 nm. The change in the UV spectrum is representative for this class of α-keto carbamates and is consistent with photocyclization to the conjugated benzo[b]furan taking place in the solid state. This spectral change is accompanied by bleaching of the deep UV π-π* absorption in the region 250-265 nm. Such bleaching is desirable in many applications and many of these base photogenerators hold significant promise as photocatalysts particularly in thick film applications where photobleaching at the exposure wavelength is critical.

Furthermore, the similarity between the solid state and the solution photolyses, as monitored by IR and UV spectroscopy implies the photochemistry is not appreciably altered in the solid state. This consideration is of importance in extending the utility of these base photogenerators to a variety of solid state applications.

iii) Photochemistry of 2,2'-Di-substituted α-Keto Carbamates

Based on the results of monitoring the photodecomposition of this class of α-keto carbamates in solution, the solid state photocyclization of these materials was not investigated in sufficient detail to warrant further discussion at this time.

3) Quantum Yield

In order to determine the photoefficiency of base photogeneration from α-keto carbamates, the standard equation (Eq. 1) defining quantum yield was rearranged to a more convenient form (Eq. 2). This equation expresses the photoefficiency of the benzoin photocyclization in a manner that allows the quantum yield to be evaluated experimentally.

$$\Phi = \frac{\text{moles of } \alpha \text{-keto carbamate consumed}}{\text{einsteins absorbed}} \quad \text{Equation 1}$$

$$\Phi = \frac{\text{starting film concentration (mol} \cdot \text{cm}^{-2}) \times \% \text{ conversion}}{\text{radiation flux (einsteins} \cdot \text{s}^{-1} \cdot \text{cm}^{-2}) \times \text{time (s)} \times \% \text{ absorbed}} \qquad \text{Equation 2}$$

In the interest of evaluating the quantum yield for photocyclization over a range of common UV exposures wavelengths we were most interested in looking at α-keto carbamates which possessed favorable UV characteristics in the range 250-400 nm. In this regard, 3,3',5,5'-tetramethoxybenzoin cyclohexyl carbamate (2) was considered a particularly attractive candidate because it possessed a weak but bleachable UV absorption maxima which extended beyond 350 nm. Accordingly, the solid state quantum yield for the photodecomposition of 3,3',5,5'-tetramethoxybenzoin cyclohexyl carbamate (2) was evaluated at 254, 313, 336 and 365 nm, as described in the Experimental Section. The quantum yields are shown in Table 2 and range between 0.05 and 0.07. In strict terms, these quantum yields are for the disappearance of the starting α-keto carbamate (2). However, the quantum yields may be assumed to be representative of cyclohexylamine photogeneration. This assumption is considered valid because carbamate (2) has demonstrated clean generation of cyclohexylamine and benzo[b]furan, uncomplicated by side products, based on ^{1}H NMR analysis of solution photolysates at low conversion. The quantum yields were evaluated at low % conversion (5-25%) by back extrapolating a plot of log quantum yield against number of quanta absorbed, to the point of zero quanta absorbed. Figure 8 illustrates the result of the quantum yield determination performed on 365 nm irradiation. Considering the limited sensitivity of the quantitative infrared technique for measuring such low % conversion values, the quantum yields at 254, 313, 336 and 365 nm are in excellent agreement within experimental error. The overall quantum yield may be assumed to be ca. 0.06 and is largely independent of exposure wavelength. Assuming that photocyclization only proceeds through direct excitation of the keto carbonyl group then a more significant variation in quantum yield would be expected on 254 nm (aryl π-π^* excitation) versus 365 nm (carbonyl n-π^* excitation) exposure. The fact that the quantum yield is not significantly affected by the exposure wavelength suggests energy transfer within the molecule is particularly efficient and that photodecomposition proceeds via different mechanisms depending on the exposure wavelength. Since GC-MS product studies on the photolysis of 3,3',5,5'-tetramethoxybenzoin cyclohexyl carbamate (2) indicate that the same products are formed on 254, 313, 336, and 365 nm photolysis, it seems likely that the photocyclization proceeds via the same excited keto moiety. This

being the case, exposure beyond 300 nm likely proceeds via direct carbonyl n-π* excitation. On the other hand, exposure at 254 nm likely involves some secondary energy transfer from the excited 3,5-dimethoxyphenyl moiety to the keto carbonyl group.

The solid state quantum yield of ca. 0.06 for amine photogeneration is significantly lower than that observed for the photoliberation of acetate and phosphate in solution[17,19,20]. This result can be rationalized as follows. First, reduced molecular motion in the solid state probably increases the difficulty of attaining appropriate conformations for photoreaction. Second, phosphate and acetate are significantly better leaving groups than the carbamoyloxy moiety.

In the case of benzoin phosphate, photocleavage is quenched by common triplet quenchers indicating that the reaction proceeds via the triplet manifold. On the other hand, the photocleavage of carboxylate and phosphate esters of meta methoxy activated benzoins is not quenched by naphthalene. This suggests the photocleavage in such systems proceeds via a singlet excited state or via a short lived triplet state. Based on the available mechanistic data, Givens *et. al.*[19] have proposed an ion-pair mechanism to explain the photocyclization of desyl phosphate esters. This mechanism may be extended to rationalize the photogeneration of amines from 3',5'-dimethoxybenzoin carbamates, as shown in Scheme 3. On irradiation, n-π* excitation of the carbonyl group leads to formation of the excited triplet state (**8**). Subsequent homolysis produces a radical pair (**9**) which undergoes rapid electron transfer to yield an ion pair (**10**). After ring closure, the liberated anion acts as a base. This base removes the bridgehead proton from (**11**), forming the benzo[b]furan photoproduct. The unstable carboxylated amine then loses carbon dioxide, liberating the free amine. The benzylic carbocation intermediate (**10**) is postulated based on the photochemical meta effect[21]. In the photochemically excited state, meta methoxy groups are known to be particularly efficient in stabilization of a developing positive charge in a benzylic site. In methoxy substituted benzenes, the electron density meta to the methoxy substituents is enhanced in the photochemical excited state. In contrast, a significantly lower electron density exists at the meta sites in the ground state. Since the photocyclization pathway is the preferred mode of photocleavage for 3',5'-dimethoxybenzoinyl carbamates, it seems probable that photocyclization proceeds via a meta benzylic carbocation as shown in Scheme 3. However, since photocleavage of the related phenacyl protecting group[15] is known to proceed by C-O homolysis followed by radical combination, this mechanism should also be considered. In this case, the benzoinyl radical formed by homolysis

13

abstracts a hydrogen atom from the solvent to give a deoxybenzoin product. Indeed, a small amount of a deoxybenzoin product (**2b**) was isolated from the photolysate from 3',5'-dimethoxybenzoin carbamate (**2**). This indicates the C-O homolysis / radical combination mechanism is only a minor photocleavage pathway. Rather, the major photocleavage pathway requires that the benzoinyl radical (**9**) preferentially undergoes rapid electron transfer to give an ion pair (**10**) which reacts as shown in Scheme 3. Similar mechanistic pathways involving competition between pure homolysis and combined homo- / heterolytic cleavage have recently been shown to be important in the photochemistry of meta methoxy benzylic esters[22].

Similar mechanistic arguments may also be used to explain the enhanced photocyclization yields in meta methoxy substituted benzoinyl carboxylate esters. In contrast, the photochemistry afforded by benzoinyl phosphate seems to be unique in undergoing efficient photocyclization without meta stabilization. This indicates the nature of the leaving group as well as the structure of the benzoinyl chromophore play an integral role in determining the photocleavage mechanism of substituted benzoins.

4) Thermal Stability

For benzoin carbamates to be potentially useful in the formulation of resist materials or imaging systems, they must be thermally stable under standard lithographic processing conditions that may include prolonged heating at temperatures upwards of 150°C. The thermal properties of these α-keto carbamates was determined by a combination of differential scanning calorimetry (DSC) and thermogravimetric analysis (TGA). As shown in Table 3, this requirement was generally fulfilled for carbamates derived from α-hydroxy ketones. This is further illustrated by the DSC curve for carbamate (**2**) (Figure 9), which shows an exotherm at 118°C corresponding to the melting point of the material. The decomposition temperature was determined by TGA, which shows that near quantitative weight loss occurs on heating carbamate (**2**) above 290°C in a nitrogen atmosphere (Figure 10). In an air atmosphere, the decomposition temperature is approximately 60°C lower for carbamate (**2**) (Table 3). Furthermore, it is known that many common photoacid generators exhibit decreased thermal stability in a phenolic matrix[23]. In contrast, these base photogenerators retain their thermal stability in a phenolic environment. For instance, both the melting point and decomposition temperature of carbamate (**2**) were only lowered by 5°C on mixing with poly(vinyl phenol) as determined by DSC. Because of their thermal

14

stability, these materials offer a potential advantage over many common photocatalysts used in microlithography and polymer curing applications.

Conclusions.

Substituted benzoin carbamate derivatives of amines show great potential as photoprecursors of organic bases. These α-keto carbamates are cleaved by UV irradiation below 370 nm down to the deep UV both in solution and in the solid state. The substitution pattern on the aryl rings and at the 2-position was varied to determine the optimal chromophore structure. Cyclohexyl carbamates derived from 3',5'-dimethoxybenzoin and its substituted analogs were particularly photoefficient affording high yields of free cyclohexylamine and the corresponding substituted benzo[b]furan as determined by ^{1}H NMR spectroscopy and GC-MS product studies. The photocleavage for this class of substituted carbamates proved particularly clean, affording minimal side products. In contrast the photochemistry of the o-nitrobenzyl class of photobase generators is particularly complex. The parent benzoinyl cyclohexyl carbamate and 2,2'-disubstituted α-keto carbamates also formed cyclohexylamine, but the photocleavage was complicated by other photoproducts besides the expected benzo[b]furan. The solid state quantum yield for the photogeneration of cyclohexylamine from the cyclohexyl carbamate of 3,3',5,5'-tetramethoxybenzoin was found to be ca.0.06 over the range 250 to 370 nm. In terms of photoefficiency, these materials are less efficient than the best o-nitrobenzyl carbamates. However, many of the 3',5'-dmethoxybenzoinyl carbamates offer a significant advantage in that they are photobleachable. The combination of clean photochemistry and photobleachable absorption makes this class of base photogenerator ideally suited to thick film applications. These materials are currently being evaluated in a number of applications requiring base photogeneration. These include polymer crosslinking for imaging and curing, and polymer modification reactions of utility in coatings, microlithography and other imaging applications.

Experimental Procedures.

General Procedures

Melting points and boiling points are uncorrected; melting points were recorded on a Gallenkamp melting point instrument. Unless stated otherwise, infrared spectra were obtained as KBr Disks using a

Nicolet FTIR/44 spectrometer. Ultraviolet-visible spectra were measured in acetonitrile solution using a Hewlett-Packard 8450 Diode Array Spectrophotometer. NMR spectra were recorded in CDCl$_3$ on a Bruker AF250 spectrometer using tetramethylsilane as internal standard. DSC was performed using a Perkin Elmer cell. TGA was performed on a Perkin Elmer thermobalance. Both techniques used a heating rate of 10°C/min. GC was performed on a Hewlett-Packard 5890 Series II Gas Chromatograph equipped with a 5% phenyl methyl silicone fused silica capillary column operating in split injection mode. GC-MS was performed on a Hewlett-Packard GC interfaced to a Hewlett Packard mass-selective detector. Solution photolyses were performed in a Rayonet Photochemical Reactor RPR100 equipped with 16 RPR3500Å lamps. Microanalyses were performed by Desert Analytics, Tucson, AZ.

Quantum Yield Determination

a) Sample Preparation

The samples used to determine quantum yields were prepared in the following manner. Poly(methacrylonitrile) (PMAN) (11.0 wt %) was dissolved in nitromethane. The polymer solution was filtered through a 0.45μm Acrodisc-PTFE filter and diluted with nitromethane to 8.91 wt %. Approximately 5.36 mol % (relative to polymer) of 3,3',5,5'-tetramethoxybenzoin cyclohexyl carbamate (**2**) was added and the solution stirred until the carbamate dissolved. The resulting solution was applied to standard silicon, sodium chloride and quartz substrates with a Headway Research Spin-coater. All films were dried at 90°C for 15 min. and then in vacuo for 12h. Film thicknesses were measured on a Tencor Alpha Step 200 and were in the range 1.1-1.3μm

b) Evaluation of Quantum Yield

In order to evaluate the quantum yield for the benzoin photocyclization, all the terms in Eq. 2 must be determined. This was achieved in the following manner. UV spectra of the sample films on quartz disks were recorded on a Hewlett Packard 8450A spectrophotometer. Thus by knowing the film absorbance and the extinction coefficient, the starting film concentration for each sample could be determined by using the Beer-Lambert law (Eqns 3-5) where A is absorbance, I_0 is the incident radiant flux, I_t is the transmitted radiant flux, ε is the molar extinction coefficient (L mol^{-1} cm^{-1}), c is concentration (mol L^{-1}), and l is the path length (cm).

$$A = \log_{10}\left(\frac{I_o}{I_t}\right) = \mathcal{E}cl \quad \text{Equation 3}$$

$$cl = \frac{A}{\mathcal{E}} \quad \text{Equation 4}$$

$$\text{starting film concentration} = \frac{cl}{1000} = \frac{A}{1000\mathcal{E}} \quad \text{Equation 5}$$

The changes in the infrared absorbance spectrum of the sample films coated on sodium chloride disks were monitored by quantitative infrared spectroscopy. This was done with use of a Nicolet FTIR/44 spectrometer equipped with software for quantitative analysis. The photochemical rearrangement was followed by monitoring the disappearance of both the keto carbonyl stretch at 1700 cm^{-1} and the carbamate carbonyl stretch at 1716 cm^{-1} in relation to the polymer reference band. The polymer reference band used was the C-H stretch at 3050-2800 cm^{-1}. The ratio (C=O/C-H) of the peak under area under the carbonyl absorption and the reference C-H absorption was calculated initially and then again after each successive UV exposure dose. The ratio of the amount of desyl substrate present after irradiation to the amount present initially multiplied by one hundred gives the percent desyl substrate remaining after exposure (Eq. 6).

$$\% \text{ substrate remaining after exposure} = \frac{\text{final (area C = O band/area C - H band)}}{\text{initial (area C = O band/area C - H band)}} \times \frac{100}{1} \quad \text{Equation 6}$$

$$\% \text{ conversion of substrate} = 100 - \% \text{ substrate remaining} \quad \text{Equation 7}$$

From this, the percent conversion caused by each exposure was found by subtraction (Eq. 7). For each exposure, two measurements of percent conversion were made on each disk. Conversion values between 5 and 25% were then used directly in the quantum yield calculation. At all exposure wavelengths, plots of % conversion against exposure time for 3,3',5,5'-tetramethoxybenzoin cyclohexyl carbamate (2) showed a near linear response within this region, thus implying that all the incident light was being absorbed by the substrate and therefore the inner filter effect was minimal at this extent of

17

reaction. This is illustrated for the 313 nm exposure of 3,3',5,5'-tetramethoxybenzoin cyclohexyl carbamate (2) (Figure 11).

UV exposure was performed using an OAI exposure tool in conjunction with an Oriel narrow band pass filter at the following exposure wavelengths 254, 313, 336, and 365 nm. The sample coated sodium chloride disks were placed at a distance from the lamp where the light output varied no more than 5% over the exposed region and was in the range 0.20-6.23 mW cm^{-2} depending on the exposure wavelength. The radiation flux at each exposure wavelength was calculated by dividing the light intensity by the energy of one einstein of irradiation at that particular wavelength. Exposure times were obtained directly from an OAI exposure timer.

The percent absorbed is the amount of light absorbed by the sample film at that particular exposure wavelength and was calculated by setting the value for the incident light equal to 100% and subsequently rearranging the Beer-Lambert law (Eqns 8-11) where I_{abs} is the absorbed radiant flux.

$$I_{abs} = I_o - I_t \quad \text{Equation 8}$$

$$I_t = I_o 10^{-\varepsilon cl} \quad \text{Equation 9}$$

$$I_{abs} = I_o\left(1 - 10^{-\varepsilon cl}\right) \quad \text{Equation 10}$$

$$\% \text{ absorbed} = 100\left(1 - 10^{-A}\right)\% \quad \text{Equation 11}$$

Thus with all the terms in Eq. 3 having been evaluated, the quantum yield at each exposure wavelength was calculated for several exposure doses. A plot of log quantum yield against the number of quanta absorbed was then used to determine the absolute quantum yield by back extrapolation to zero quanta absorbed. This method of determination corrects for any internal filtering by the benzofuran photo by-product. This procedure was used to calculate the quantum yield for photocyclization of 3,3',5,5'-tetramethoxybenzoin cyclohexyl carbamate (2) at 254, 313, 336 and 365 nm.

Preparative Photolysis

Photogeneration of Cyclohexylamine and Preparation of 2-(3,5-Dimethoxyphenyl)-5,7-dimethoxybenzo[b]furan (2a).

A pyrex flask containing a solution of carbamate (**2**) (0.234g, 0.512mmol) in dry, degassed acetonitrile (100ml) was irradiated for 2h in a Rayonet photolysis chamber fitted with 350 nm lamps. During this time, samples were removed and monitored by GC which indicated that cyclohexylamine was being liberated. After 2h, TLC confirmed the formation of one major photoproduct along with other trace polar photoproducts. The solvent was removed in vacuo and the residual oil purified by flash chromatography (10% ethyl acetate / 90% hexane) to give 2-(3,5-dimethoxyphenyl)-5,7-dimethoxybenzo[b]furan (**2a**) as a white solid (0.137g, 85%). An analytically pure sample was obtained by recrystallization from ethyl acetate-hexane.

M.p. 106-108°C (Lit.[20] m.p. 110-111°C). Microanalysis: Calculated for $C_{18}H_{18}O_5$ (314.32); C 68.78, H 5.77; Found C 68.58, H 5.46%. UV: $\varepsilon_{(286sh)}24205$, $\varepsilon_{(300)}28727$, $\varepsilon_{(318sh)}19136$. IR v 1611, 1602, 1594, 1491, 1342, 1204, 1160, 1149, 1036, 824 cm^{-1}. ^{1}H NMR δ 3.86 and 4.02 (each 3H, each s, Ar(1) 5,7-OCH$_3$), 3.88 (6H, s, Ar(2) 3,5-OCH$_3$), 6.47 (1H, t(J$_m$=2.2Hz), Ph 4-H), 6.48 (1H, d(J$_m$=2.2Hz), Bf 6-H), 6.63 (1H, d(J$_m$=2.2Hz), Bf 4-H), 6.95 (1H, s, Bf 3-H), 7.03 ppm (2H, d(J$_m$=2.2Hz), Ph 2,6-H). ^{13}C NMR δ 55.52 (q), 56.08 (q), 55.83 (q), 94.37 (d), 97.34 (d), 100.95 (d), 102.45 (d), 102.99 (d), 130.38 (s), 132.15 (s), 139.37 (s), 145.44 (s), 156.31 (s), 156.86 (s), 161.00 (s) ppm.

Further elution of the column allowed isolation of one minor photoproduct as a yellow oil (0.011g, 7%). This material was tentatively identified as 1-(3,5-dimethoxyphenyl)-2-(3,5-dimethoxyphenyl)ethanone (**2b**) by ^{1}H NMR spectroscopy.

^{1}H NMR δ 3.77 and 3.83 (each 6H, each s, Ar(1) and Ar(2) 3,3',5,5'-OCH$_3$), 4.18 (2H, s, 2-CH$_2$), 6.37 (1H, t(J$_m$=2.2Hz), Ar(2) 4-H), 6.43 (2H, d(J$_m$=2.2Hz), Ar(2) 2,6-H), 6.65 (1H, t(J$_m$=2.2Hz), Ar(1) 4-H), 7.16 ppm (2H, d(J$_m$=2.2Hz), Ar(1) 2,6-H).

Photogeneration of Cyclohexylamine and Preparation of 2-phenyl-5,7-dimethoxybenzo[b]furan (3a).

A pyrex flask containing a solution of carbamate (**3**) (0.196g, 0.493mmol) in dry degassed acetonitrile (100ml) was irradiated for 2h in a Rayonet photolysis chamber fitted with 350nm lamps.

During this time samples were removed and monitored by GC which indicated that cyclohexylamine was being liberated. After 2h, TLC confirmed the formation of one major photoproduct along with other trace polar photoproducts. The solvent was removed in vacuo and the residual oil purified by flash chromatography (10% ethyl acetate / 90% hexane) to give 2-phenyl-5,7-dimethoxybenzo[b]furan (**3a**) as a white solid (0.100g, 80%). An analytically pure sample was obtained by recrystallization from hexane. M.p. 68-69°C (Lit.[17] m.p. 89.1-89.6°C). Microanalysis: Calculated for $C_{16}H_{14}O_3$ (254.27): C 75.57, H 5.55; Found C 75.50, H 5.30%. UV: $\varepsilon_{(246)}9301$, $\varepsilon_{(292sh)}25067$, $\varepsilon_{(300)}25817$, $\varepsilon_{(317sh)}15855$. IR ν 1606, 1479, 1429, 1594, 1218, 1214, 1147, 824, 765, 761 cm^{-1}. ^{1}H NMR δ 3.87 and 4.03 (each 3H, each s, Ar(1) 5,7-OCH$_3$), 6.47 (1H, d(J$_m$=2.2Hz), Bf 6-H), 6.64 (1H, d(J$_m$=2.2Hz), Bf 4-H), 6.97 (1H, s, Bf 3-H), 7.35 (1H, m approximates to t, Ph 4-H), 7.43 (2H, m approximates to dt, Ph 3,5-H), 7.88 ppm (2H, m approximates to d, Ph 2,6-H). ^{13}C NMR δ 55.11 (q), 55.83 (q), 94.35 (d), 97.21 (d), 101.87 (d), 124.92 (d), 128.46 (d), 128.69 (d), 130.36 (s), 130.49 (s), 139.42 (s), 145.48 (s), 156.49 (s), 156.84 (s) ppm.

References.

1. B.Amit, U. Zehavi and A.Patchornik, *Isr. J. Chem.* **1974**, *12*, 103; U. Zehavi, *Adv. Carbohydr. Chem. Biochem.*, **1988**, *46*, 179.

2. S.A. MacDonald, C.G. Willson and J.M.J. Fréchet, *Acc. Chem. Res.*, **1994**, *27*, 151. J.M.J. Fréchet, J.M. Havard, S. M. Lee, S.Y. Shim, E.J. Urankar; *Polym. Mat. Sci. Eng.*, **1995**, *72*, 4. C.G. Willson; H. Ito; J.M.J. Fréchet; T.G. Tessier; F.M. Houlihan. *J. Electrochem. Soc.* **1986**, *133*, 181-187.

3. J.M.J. Fréchet; H. Ito; C.G. Willson, *Proc. Microcircuit Eng.* **1982**, 260. Fréchet, J. M. J.; Eichler, E.; Ito, H.; Willson, C. G. *Polymer* **1983**, *24*, 995-1000.. Ito, H.; Willson, C. G.; Fréchet, J. M. J. US. Patent 4,491,628; 1985.

4. J.G. Maltabes.; Holmes, S. J.; Morrow, J. R.; Barr, R. L.; Hakey, M.; Reynolds, G.; Brunsvold, W. R.; Willson, C. G.; Clecak, N. J.; MacDonald, S. A.; Ito, H. Advances in Resist Technology and Processing VII. *Proc. SPIE* **1990**, *1262*, 2-7. S. Holmes; R. Levey, ; A. Bergendahl.; K. Holland; J. Maltabes.; S. Knight.; K.C. Korris.; D. Poley. Optical/Laser Microlithography III. *Proc. SPIE* **1990**, *1264*, 61-70.

5. A.M. Gurnery and H.A. Lester, *Physiol. Rev.*, **1987**, *67*, 583; J.A. McCray and D.R. Trentham, *Annu. Rev. Biophys. Biophys. Chem.*, **1989**, *18*, 239.

6. S.P.A. Fodor, J. Leighton-Read, M.C. Pirrung, L. Stryer, A. Tsui Lu, and D. Solas, *Science*, **1991**, *251*, 767, L.F. Rozsnayai, D.R. Benson, S.P.A. Fodor, and P.G. Schultz, *Angew. Chem. Int . Ed. Engl.*, **1992**, *31*, 759, G. von Kiederowski, *Angew. Chem. Int . Ed. Engl.*, **1991**, *30*, 822; A.C. Pease, D. Solas, E.J. Sullivan, M.T. Cronin, C.P. Holmes and S.P.A. Fodor, *Proc. Natl. Acad. Sci. USA*, **1994**, *91*, 5022.

7. C.G. Willson *Introduction to Microlithography: Theory, Materials and Processing*, Thompson, L. F., Willson, C. G., Bowden, M. J., Eds.; ACS Symposium Series 219; American Chemical Society: Washington, DC, 1983; pp 87-159. A. Reiser, *Photoreactive Polymers: The Science and Technology of*

21

Resists, John Wiley & Sons., 1989. E. Reichmanis, *Polym. Mat. Sci. Eng.*, **1992**, *64*, 36; E. Reichmanis, F.M. Houlihan, O. Nalamasu and T.X. Neenan, *Chem. Mater.*, **1991**, *3*, 394; A.A. Lamola, C.R.Szmanda and J.W. Thackeray, *Solid State Technol.*, **1991**, *34(8)*, 53.

8. J.M.J. Fréchet, *Pure & Applied Chemistry*, **1992**, *64*, 1239.C.R. Kutal and C.G. Willson, *J. Electrochem. Soc.*, **1987**, *134*, 2280; K.H. Song, S. Tonogai, M. Tsunooka and M.Tanaka, *J. Photochem.Photobiol. A ;Chem.* **1989**, *49*, 269.

9. J.F. Cameron and J.M.J. Fréchet, *J. Org. Chem.*, **1990**, *55*, 5919; J.F. Cameron and J.M.J. Fréchet, *J. Photochem. Photobiol. A*, **1991**, *59*, 105. J.F. Cameron and J.M.J. Fréchet, *J. Am. Chem. Soc.*, **1991**, *113*, 4303; J.F. Cameron and J.M.J. Fréchet, *Polym. Mat. Sci. Eng.*, **1991**, *64*, 55.

10. J.E. Beecher, J.F. Cameron and J.M.J. Fréchet, *Polym. Mat. Sci. Eng.*, **1991**, *64*, 71; J.E. Beecher, J.F. Cameron and J.M.J. Fréchet, *J. Mater. Chem.*, **1992**, *2*, 811.
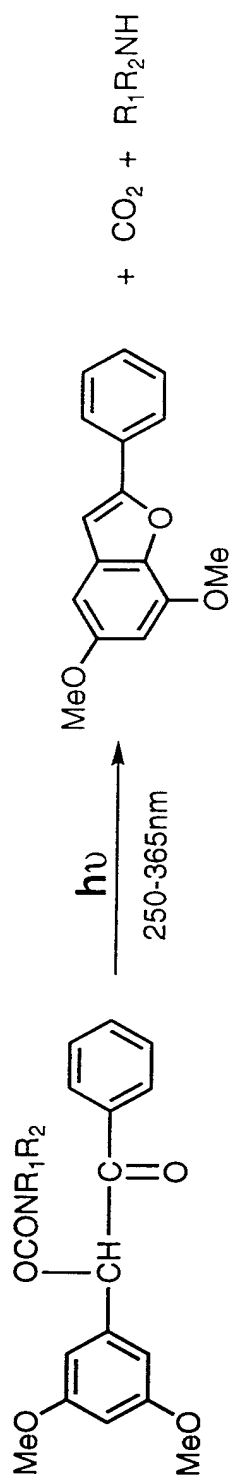
11. J.M.J. Fréchet, J.F. Cameron, C.M. Chung, S.A. Haque and C.G. Willson, *Polym. Bull.*, **1993**, *30*, 369. D.R. McKean, G.M. Wallraff, W. Volksen, N.P. Hacker, M.I. Sanchez and J.W. Labadie, *Polym. Mat. Sci. Eng.*, **1994**, *66*, 237; D.R. McKean, T Brifffaud, W. Volksen, N.P. Hacker, J.W. Labadie, *Polym. Mat. Sci. Eng.*, **1994**, *70*, 387. T. Nishikubo, E. Takehara and A. Kameyama, *Polymer J.*, **1993**, *25*, 421.

12. S. Matuszczak, J.F. Cameron, J.M.J. Fréchet and C.G. Willson, *J. Mater. Chem.*, **1991**, *1*, 1045. C.G. Willson, J.F. Cameron, S.A. MacDonald, C.P. Niesert, J.M.J. Fréchet, M.K. Leung and A. Ackmann, *Proc. S.P.I.E. Advances in Resist Technology and Processing X*, **1993**, *1925*, 354.

13. M.K. Leung, J.M.J. Fréchet, J.F. Cameron and C.G. Willson, *Polym. Mat. Sci. Eng.*, **1993** *68*, 30; C.G. Willson, J.F. Cameron, S.A. MacDonald, C.P. Niesert, J.M.J. Fréchet, M.K. Leung and A. Ackmann, *Polym. Mat. Sci. Eng.*, **1993** *68*, 60.
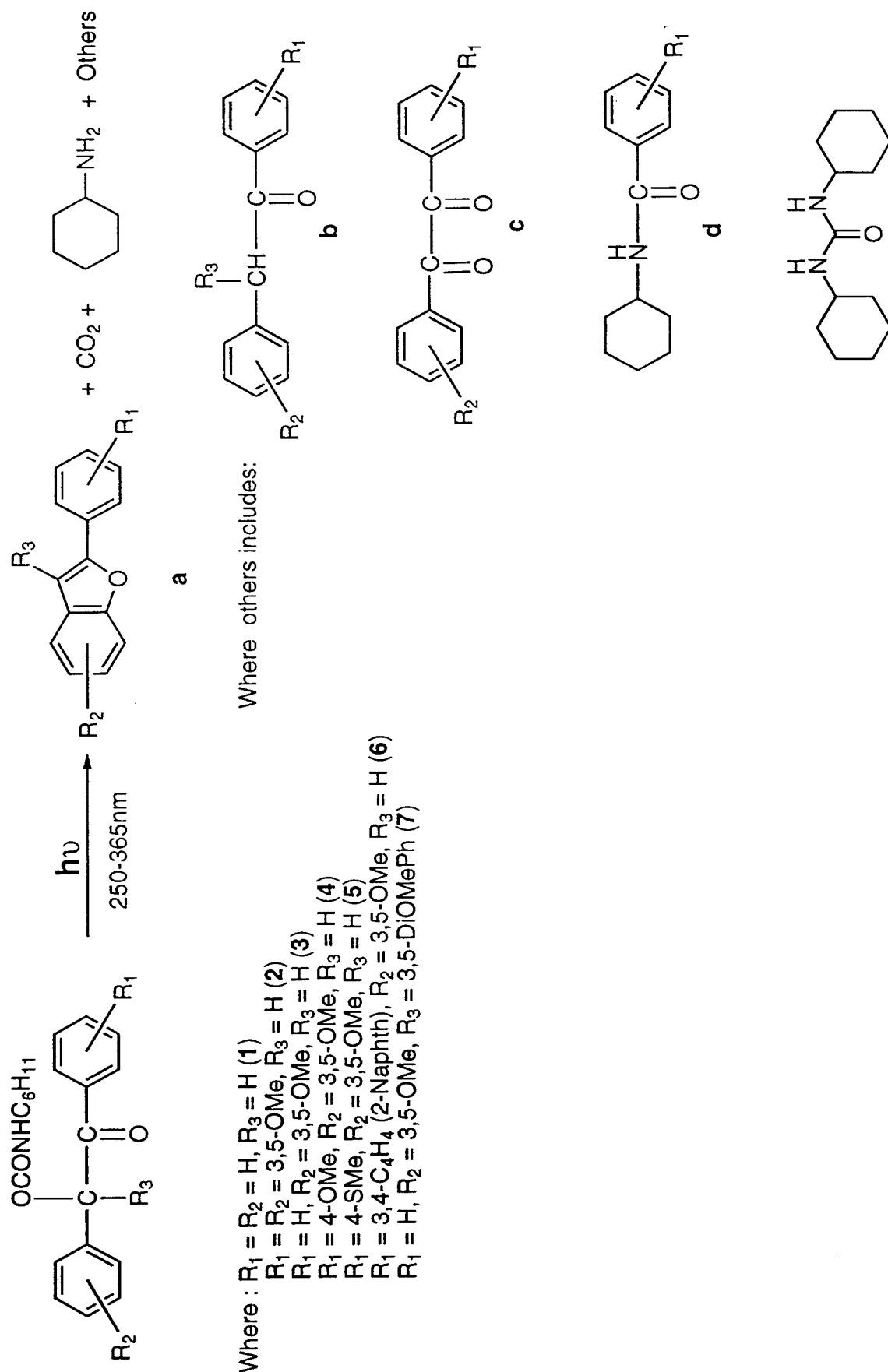
14. J.F. Cameron, C.G. Willson and J.M.J. Fréchet, *J. Chem. Soc., Chem. Commun.*, **1995**, in press; J.F. Cameron, C.G. Willson and J.M.J. Fréchet, Presented at the 209th National Meeting of the American Chemical Society, Anaheim, CA, April 1995, Paper ORGN 237.

15. J.C. Sheehan and K. Umezawa, *J. Org. Chem.*, **1973**, *38*, 3771; G. Church, J.M. Ferland and J. Gauthier, *Tetrahedron Lett.*, **1989**, *30*, 1901.

16. J.C. Sheehan and R.M. Wilson, *J. Am. Chem. Soc.*, **1964**, *86*, 5277.

17. J.C. Sheehan, R.M. Wilson and A.W. Oxford, *J. Am. Chem. Soc.*, **1971**, *93*, 7222.

18. M.R. Winkle, E.P. 0 425 142 A2, 1991.

19. R. S. Givens and B. Matuszewski, *J. Am. Chem. Soc.*, **1984**, *106*, 6860; R. S. Givens, P.S. Athey, L. William Kueper III, B. Matuszewski and J.Y. Xue, *J. Am. Chem. Soc.*, **1992**, *114*, 8708; R. S. Givens, P.S. Athey, B. Matuszewski, L. William Kueper III, J.Y. Xue and T. Fister, *J. Am. Chem. Soc.*, **1992**, *114*, 8708; R. S. Givens and L. William Kueper III, *Chem. Rev.*, **1993**, *93*, 55.

20. J.E.T. Corrie and D.R. Trentham, *J. Chem. Soc., Perkin Trans. 1*, 1992, 2409.

21. H.E. Zimmerman in *Adv. Photochem.*, W.A. Noyes Jr., G.S. Hammond and J.N. Pitts Jr., Eds, Interscience, New York, 1963, Volume 1, p.183.

22. J.A. Pincock and P.J. Wedge, *J. Org. Chem.*, 1994, **59**, 5587; J.W. Hilborn, E. MacKnight, J.A. Pincock and P.J. Wedge, *J. Am. Chem. Soc.*, 1994, **116**, 3337;

23. G.G. Barclay, D.R. Medeiros and R.F. Sinta, *Chem. Mater.*, **1995**, in press; G.G. Barclay, D.R. Medeiros and R.F. Sinta, *Polym. Mat. Sci. Eng.*, **1993**, *68*, 71.

Scheme 1

$$h\upsilon \atop 250\text{-}365\text{nm}$$

$+ \quad CO_2 \quad + \quad R_1R_2NH$

Where $R_1 = H$, $R_2 = C_6H_{11}$
R_1, $R_2 = -(CH_2)_5-$;

Scheme 2

$h\upsilon$
250-365nm

a

Where others includes:

b

c

d

Where : $R_1 = R_2 = H$, $R_3 = H$ (**1**)
$R_1 = R_2 = 3,5$-OMe, $R_3 = H$ (**2**)
$R_1 = H$, $R_2 = 3,5$-OMe, $R_3 = H$ (**3**)
$R_1 = 4$-OMe, $R_2 = 3,5$-OMe, $R_3 = H$ (**4**)
$R_1 = 4$-SMe, $R_2 = 3,5$-OMe, $R_3 = H$ (**5**)
$R_1 = 3,4$-C_4H_4 (2-Naphth), $R_2 = 3,5$-OMe, $R_3 = H$ (**6**)
$R_1 = H$, $R_2 = 3,5$-OMe, $R_3 = 3,5$-DiOMePh (**7**)

$+ CO_2 + $ $-NH_2$ + Others

Scheme 3
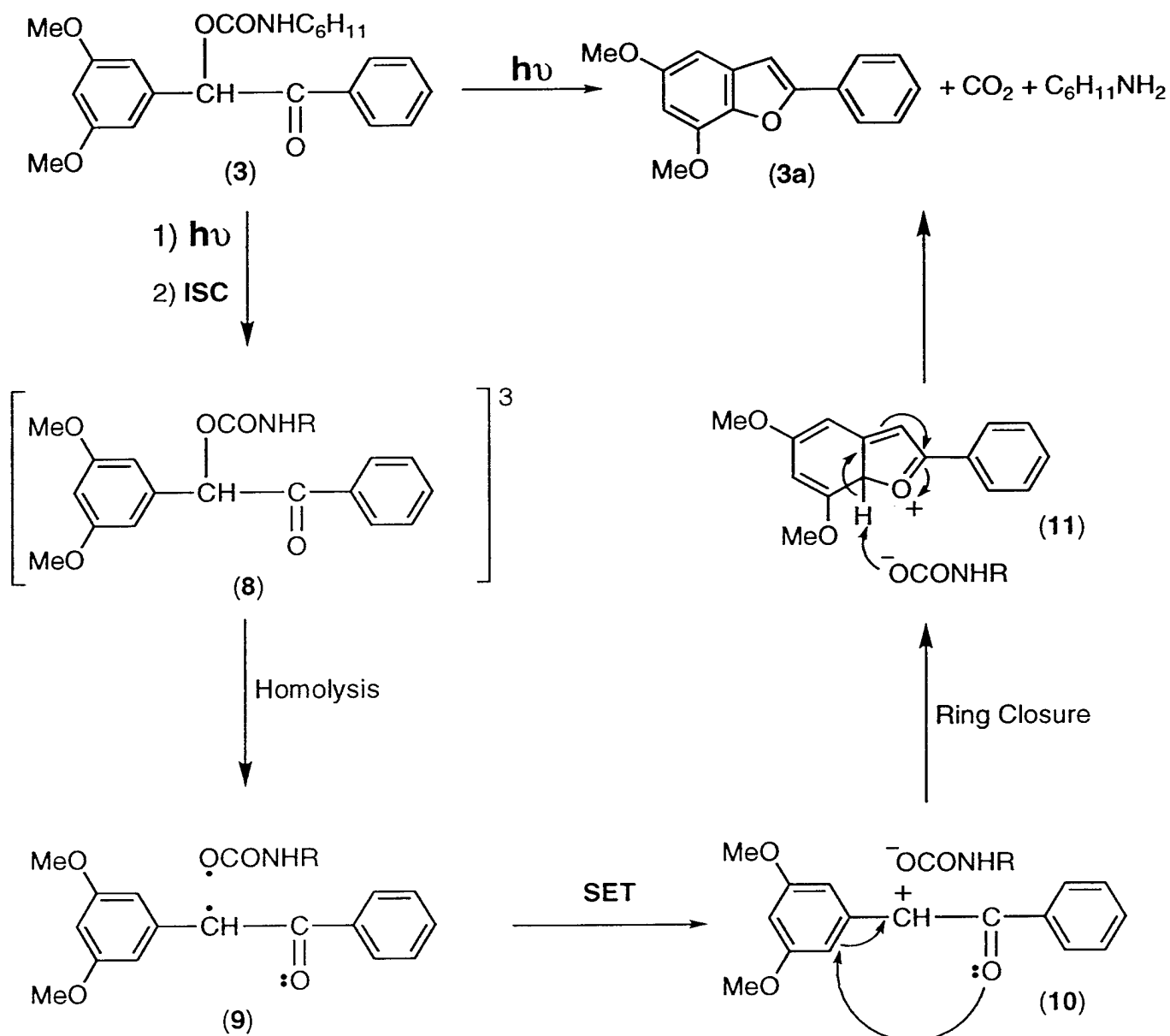
TABLE 1

NMR Monitoring of the Photogeneration Of Cyclohexylamine from Assorted Carbamates

Carbamate	% Conversion[a]	δ(3-Bf-H)[b]
Benzoin (1)	75	Not Observed
3,3',5,5'-TetraMeO (2)	87	7.14
3',5'-DiMeO (3)	93	7.12
3',4,5'-DiMeO (4)	98	6.96
3',5'-DiMeO-4-MeS (5)	37	7.07
3',5'-DiMeO-2-Naphth (6)	62	7.25
2,2-Di-(3',5'-MeO) (7)	62	Not Observed

a) % Conversion calculated from the integral ratio of the photogenerated cyclohexylamine methine (CH, m, δ 2.52) and the aromatic resonances after 60min 350nm Rayonet exposure.

b) Chemical shift for resonance of 3-H in benzofuran photoproduct in MeCN-d3 quoted ppm downfield from TMS.

TABLE 2

Quantum Yields[a] For The Photocyclization Of 3,3',5,5'-Tetramethoxybenzoin Carbamate (2) (With Concomitant Liberation of Cyclohexylamine)

Φ_{254nm}	Φ_{313nm}	Φ_{336nm}	Φ_{365nm}
0.053	0.071	0.051	0.065

a) Quantum yield evaluated from a plot of log Φ versus the number of quanta absorbed, by back extrapolation to to zero quanta absorbed, from data taken at conversion values unaffected by the inner filter effect.

TABLE 3

Thermal Properties of Substituted Benzoin Carbamates

Carbamate	Melting Point	Decomposition Temperature[a]
Benzoin (1)	87-88°C	193°C
3,3',5,5'-TetraMeO (2)	116-118°C	233°C
3',5'-DiMeO (3)	149-151°C	203°C
3',4, 5'-DiMeO (4)	105-107°C	218°C
3',5'-DiMeO-4-MeS (5)	152-154°C	252°C
3',5'-DiMeO-2-Naphth (6)	161-162°C	230°C
2,2-Di-(3',5'-MeO) (7)	170-172°C	231°C

a) Decomposition temperature was taken as the temperature of 5% weight loss as determined by Thermogravimetric Analysis (in air).

Figure Titles

Figure 1: Change in ^{1}H NMR aromatic resonances of carbamate (2) as a 38.6 mM solution in THF-d8 with increasing 350 nm photolysis in Rayonet.

a) Prior to exposure.
b) After 15min exposure.
c) After 30min exposure.
d) After 60min exposure.
e) After 90min exposure.

Figure 2: Plot of % conversion against exposure time for carbamate (2) as a 38.6 mM solution in THF-d8 on 350 nm exposure in Rayonet.

Figure 3: Change in carbonyl region of carbamate (3) as a 11.8 mM solution in MeCN with increasing 350 nm photolysis in Rayonet.

a) Prior to exposure.
b) After 5min exposure.
c) After 10min exposure.
d) After 15min exposure.
e) After 20min exposure.
f) After 30min exposure.
g) After 45min exposure.
h) After 60min exposure.
i) After 120min exposure.

Figure 4: Change in N-H stretching region of carbamate (3) as a 11.8 mM solution in MeCN with increasing 350 nm photolysis in Rayonet.

a) Prior to exposure.
b) After 5min exposure.
c) After 10min exposure.
d) After 15min exposure.
e) After 30min exposure.
f) After 60min exposure.
g) After 120min exposure.
h) After 240min exposure.

Figure 5: Change in UV spectrum of carbamate (2) as a 6.164×10^{-5}M solution in MeCN with increasing 350 nm photolysis.

a) Prior to exposure.
b) After 15s exposure.
c) After 30s exposure.
d) After 45s exposure.
e) After 75s exposure.
f) After 120s exposure.
g) After 180s exposure.
h) After 300s exposure.
i) After 450s exposure.

Figure 6: Change in IR spectrum of carbamate (2) (5.36 mol%) in a 1.265μm thick PMAN film with increasing 254 nm exposure dose.

a) Prior to exposure.
b) After 50mJcm^{-2} exposure.
c) After 100mJcm^{-2} exposure.
d) After 200mJcm^{-2} exposure.
e) After 300mJcm^{-2} exposure.
f) After 400mJcm^{-2} exposure.
g) After 500mJcm^{-2} exposure.
h) After 750mJcm^{-2} exposure.
i) After 1.0Jcm^{-2} exposure.

Figure 7: Change in UV spectrum of carbamate (3) (4.67 mol%) in a 1.375μm thick PMAN film with increasing 254 nm exposure dose.

a) Prior to exposure.
b) After 30mJcm^{-2} exposure.
c) After 75mJcm^{-2} exposure.
d) After 125mJcm^{-2} exposure.
e) After 200mJcm^{-2} exposure.
f) After 300mJcm^{-2} exposure.
g) After 500mJcm^{-2} exposure.
h) After 1.0Jcm^{-2} exposure.

Figure 8: Plot of log quantum yield against number of quanta absorbed for 365 nm exposure of carbamate (2) (5.36 mol%) in a 1.265μm thick PMAN film.

Figure 9: Differential scanning calorimetry trace for carbamate (2).

Figure 10: Thermogravimetric analysis trace for carbamate (2).

Figure 11: Plot of % conversion against exposure dose for 313 nm exposure of carbamate (2) (5.36 mol%) in a 1.265μm thick PMAN film.
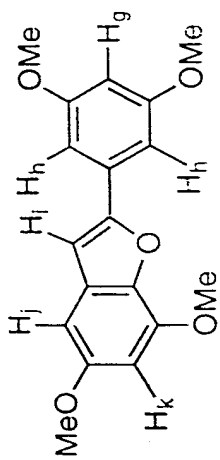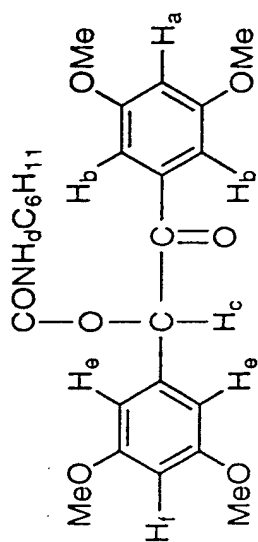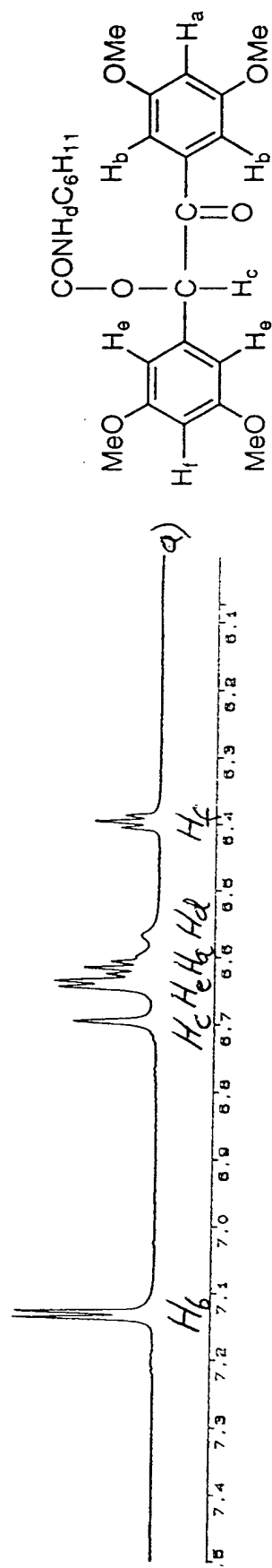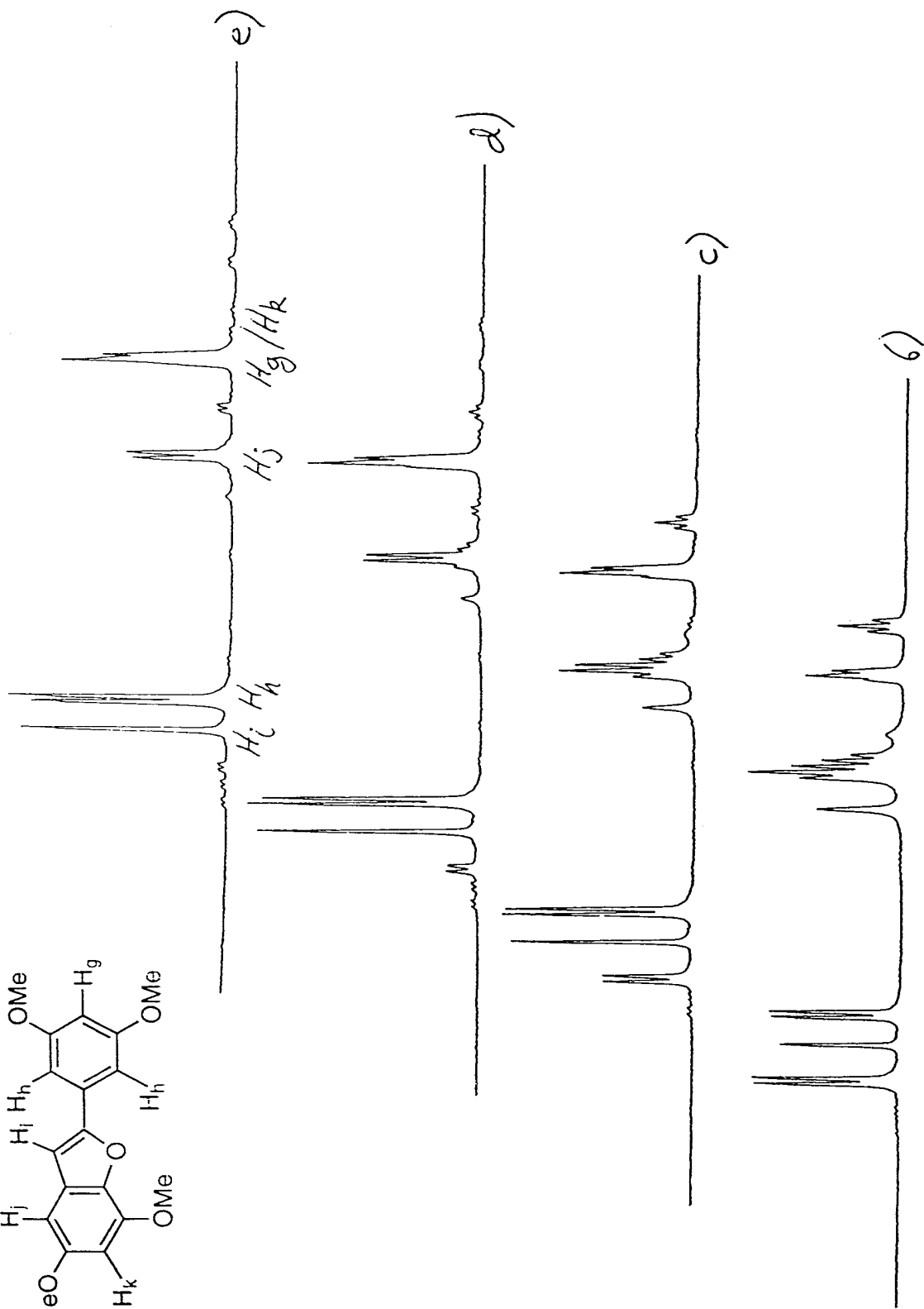
2

Fig 1

Fig 2

Fig 3

% TRANSMITTANCE

RESULT   REFERENCE   SAMPLE

a) Prior to 350nm Radiation
b) After 5min 350nm Exposure
c) "   10min "   "
d) "   15min "   "
e) "   20min "   "
f) "   30min "   "
g) "   45min "   "
h) "   60min "   "
i) "   120min "   "

WAVENUMBERS
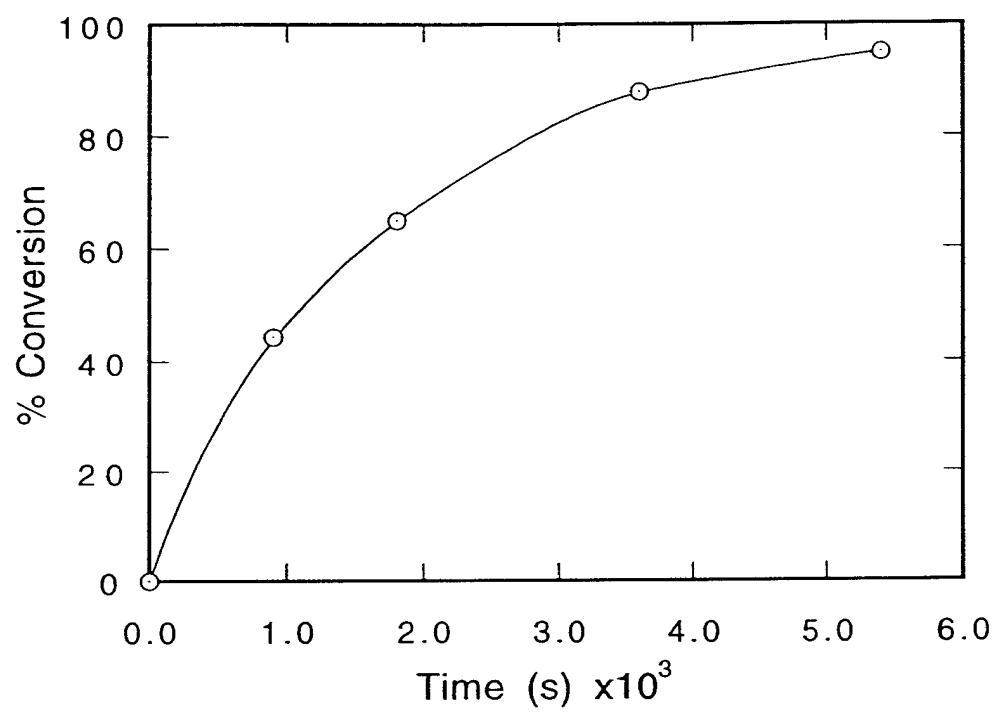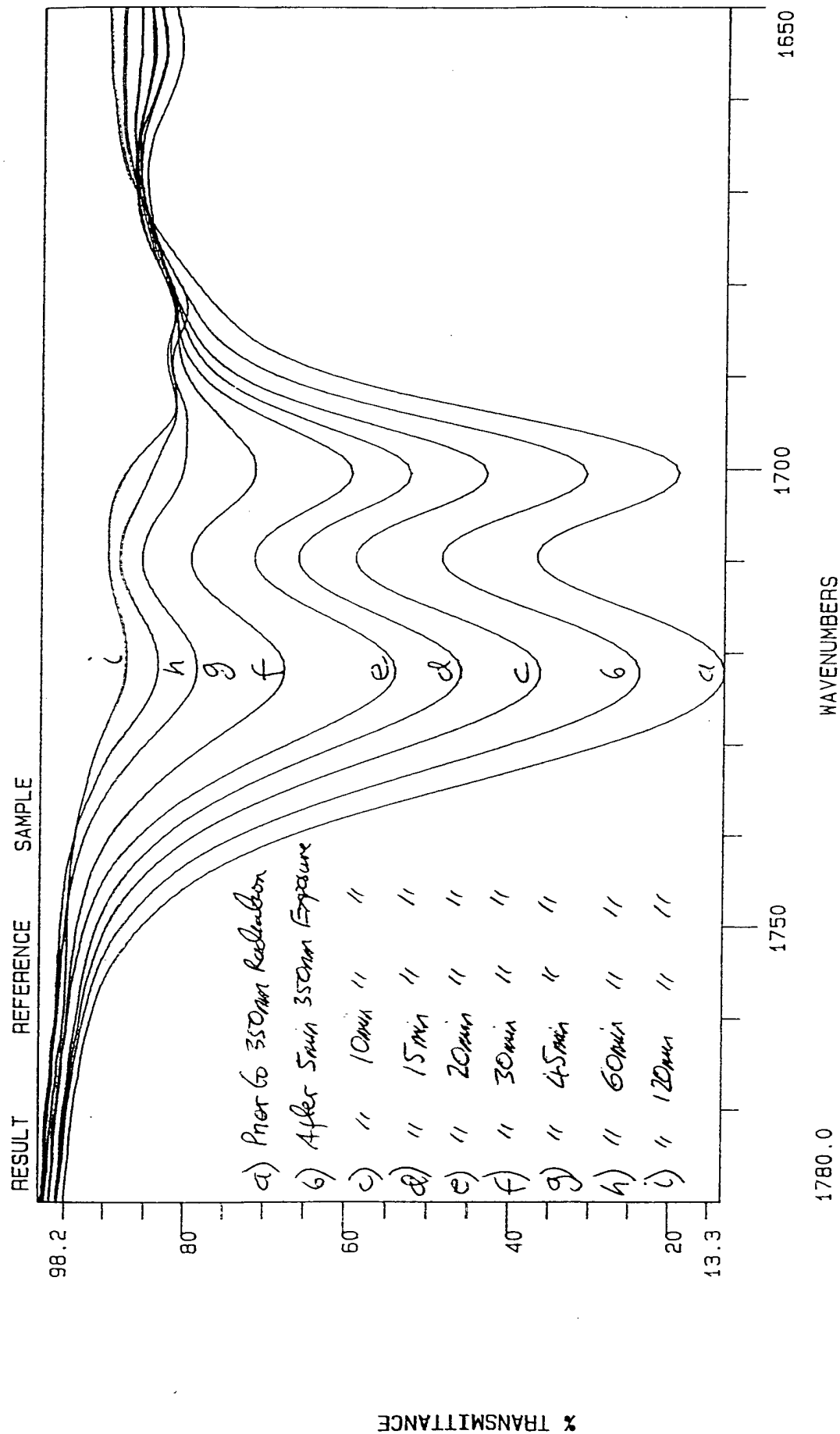
jfc1711/25a1-after 2h 350nm rayonet exposure in mecn soln

Fig 4

RESULT   REFERENCE   SAMPLE

a) Prior to 350nm Exposure
b) After 5min 350nm Exposure
c) "   10min "   "
d) "   15min "   "
e) "   30min "   "
f) "   60min "   "
g) "   120min "   "
h) "   240min "   "

PO = 19
Smoothed Spectra
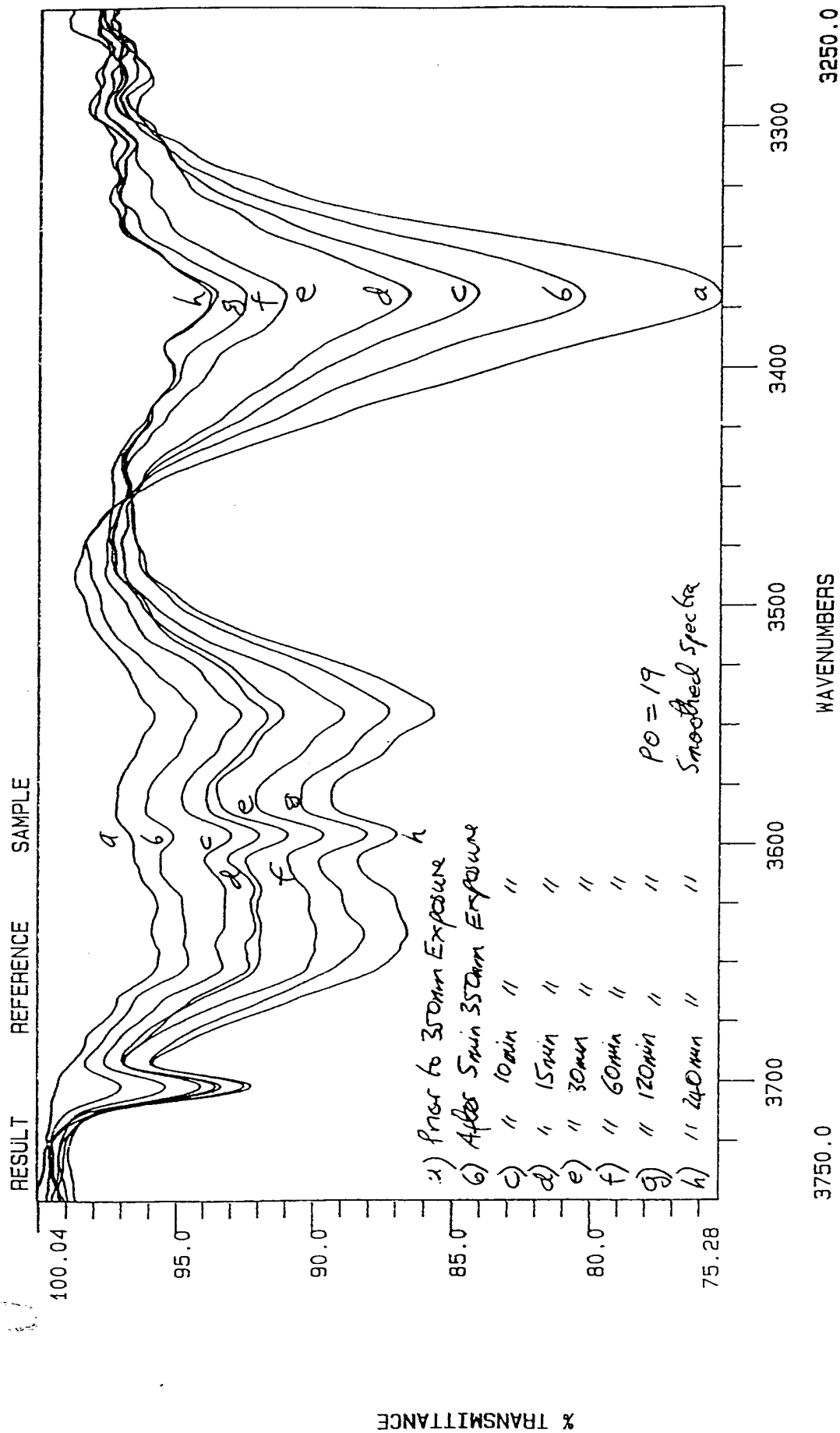
jfc1711/25a1-10min 350nm rayonet exposure of 25a1/mecn soln

% TRANSMITTANCE

WAVENUMBERS

100.04   95.0   90.0   85.0   80.0   75.28

3750.0   3700   3600   3500   3400   3300   3250.0

Fig 5

JFC1646/67A1-6.164*10-5M IN MECN,350NM RAYONET

a) Prior 6 sec. 251
b) After 1 sec. 266
c) " " 30 " 340
d) " " 45 " "
e) " " 75 " "
f) " " 120 " "
g) " " 180 " "
h) " " 300 " "
i) " " 450 " "

ABSORBANCE

WAVELENGTH (nm)

Fig 6

% TRANSMITTANCE

RESULT   REFERENCE   SAMPLE

1800   1750   1700   1650   1640.0

WAVENUMBERS

a) Prior to exposure
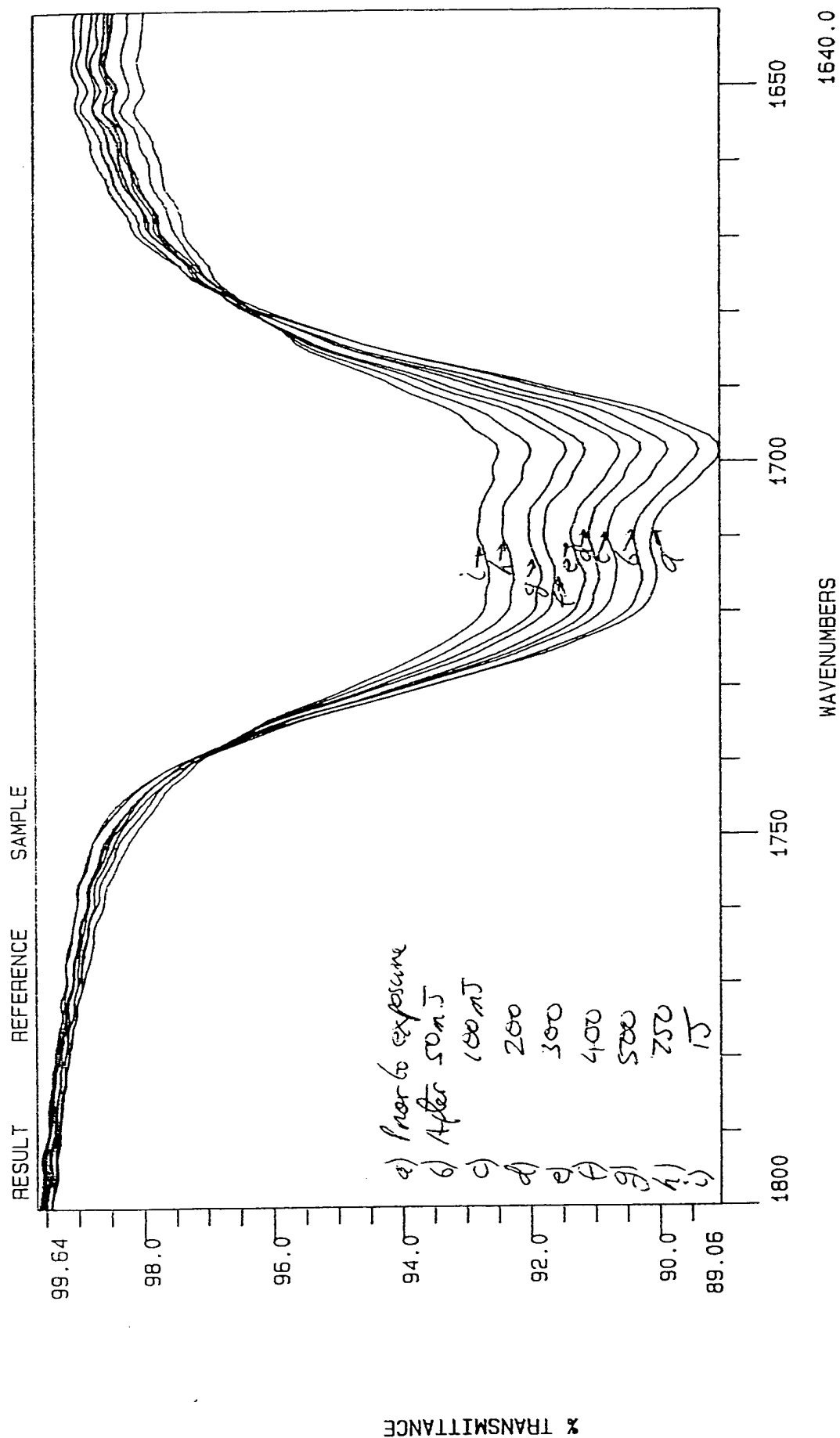b) After 50mJ
c) 100mJ
d) 200
e) 300
f) 400
g) 500
h) 750
i) 1J
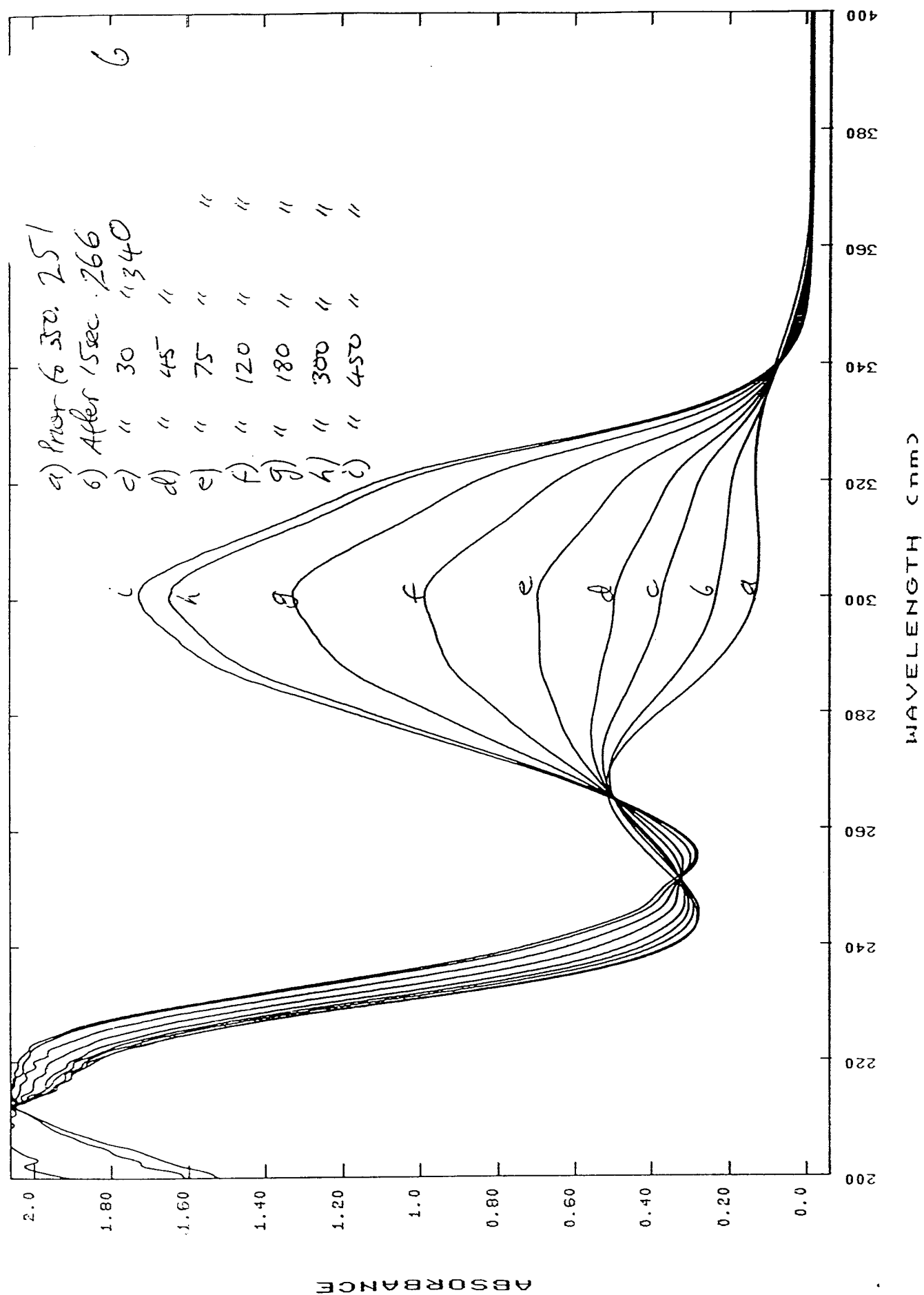
jfc1646/67a1-5 mol% in pman matrix, 1.41 micron thick
After 100mj/sqcm esposure dose at 254nm

Fig 7
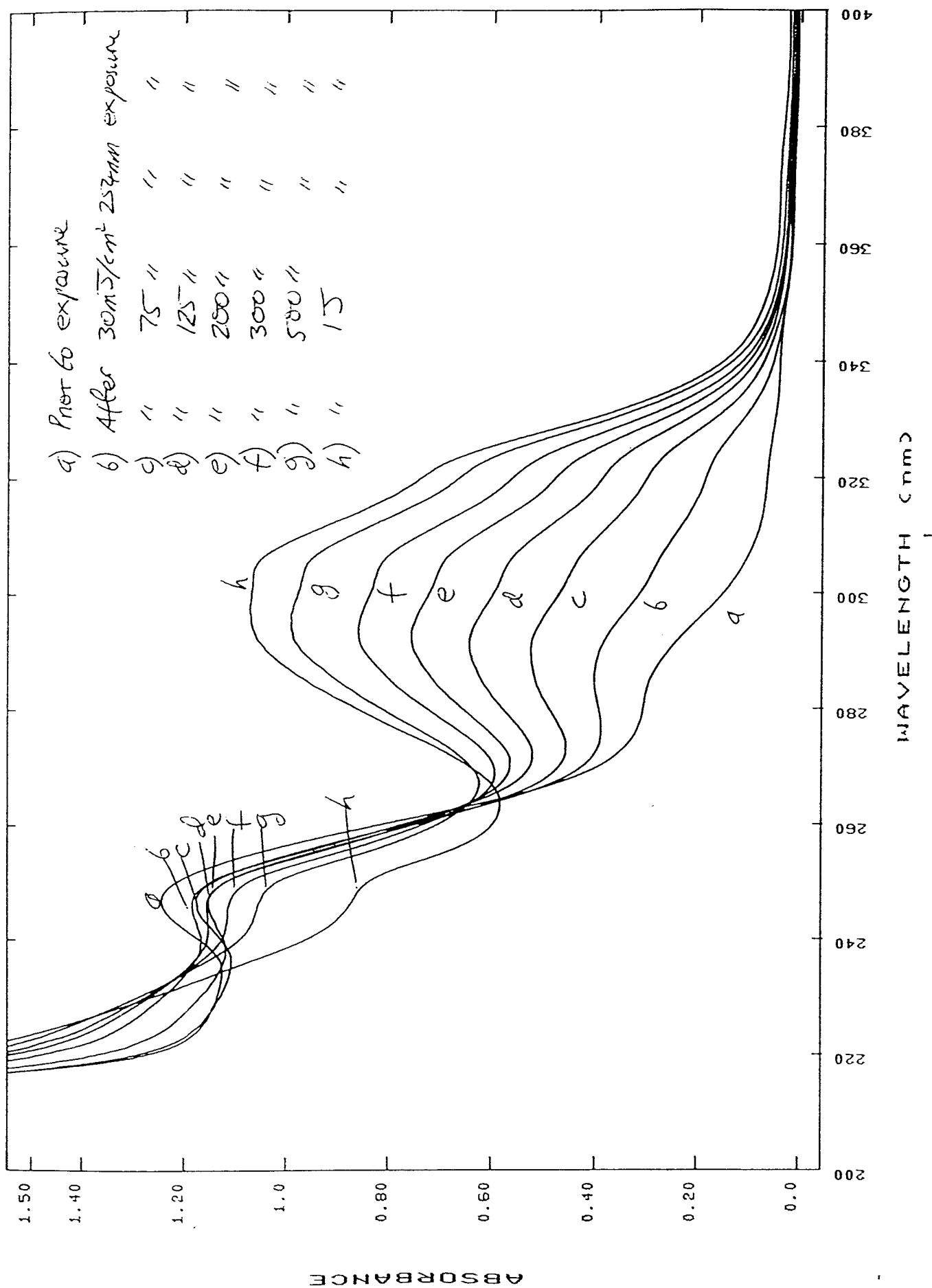
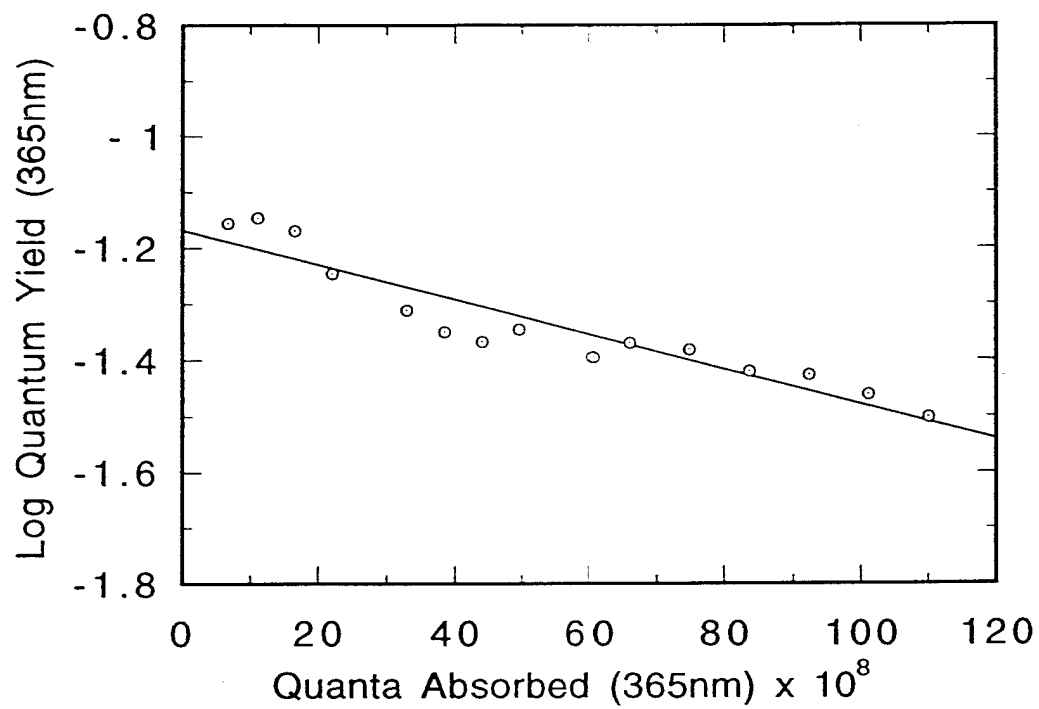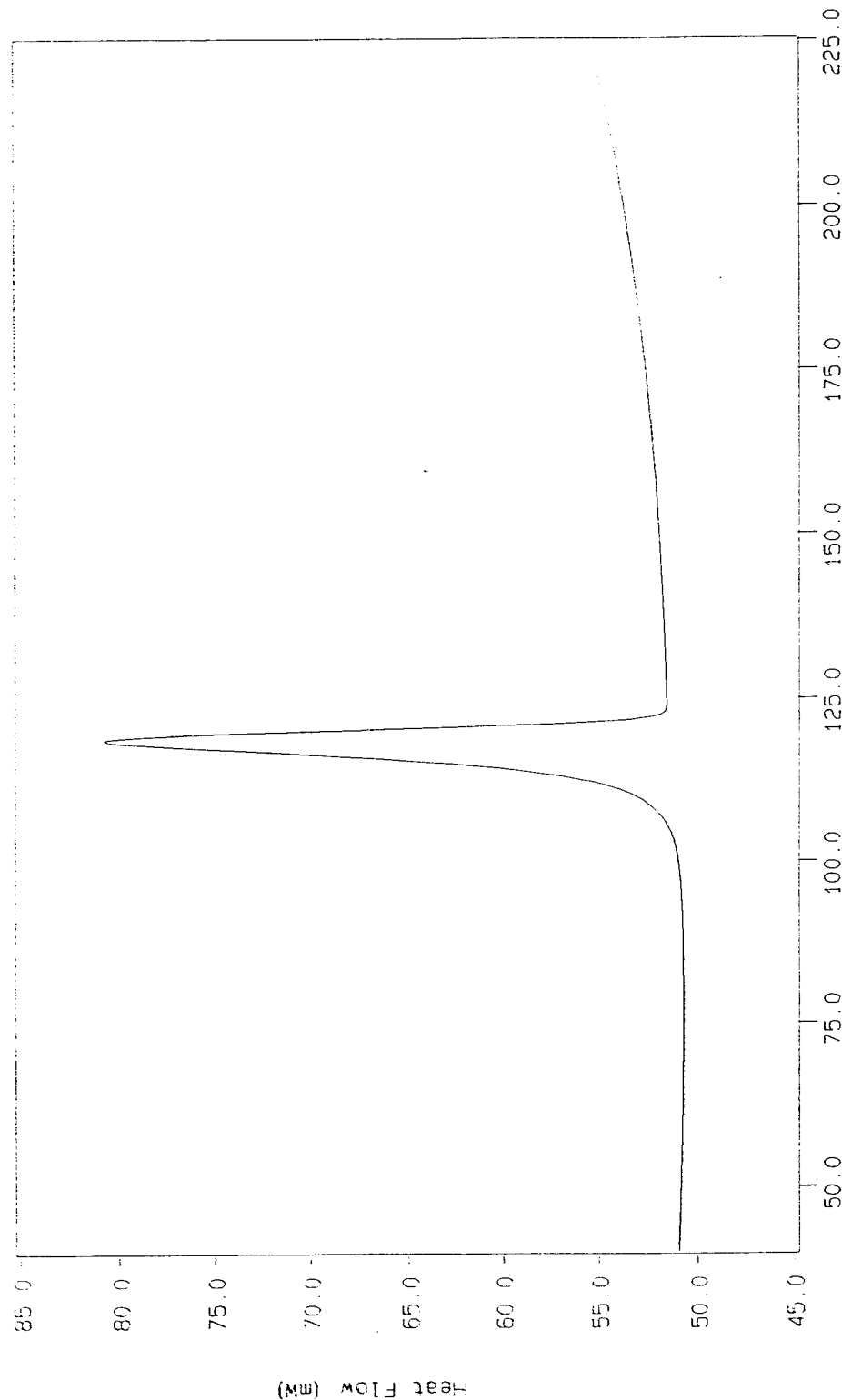JPC1/11/2SA1-4.67MOL/ IN 1.375UM PMAN FILM, 254NM EXPOSURE

a) Prior to exposure
b) After 30mJ/cm² 254nm exposure
c)   ''   75 ''   ''
d)   ''   125 ''   ''
e)   ''   200 ''   ''
f)   ''   300 ''   ''
g)   ''   500 ''   ''
h)   ''   15

ABSORBANCE

WAVELENGTH (nm)

Fig 8

Fig 9

Curve 1: DSC
File Info: JFC1646/67A1 Tue Jun 7 16:07:04 1994
Sample Weight: 4.900 mg

JFC1646/67A1

1 JFC1646/67A1

Heat Flow (mW)

Heat Flow (mW)

Temperature (°C)

85.0 80.0 75.0 70.0 65.0 60.0 55.0 50.0 45.0

50.0 75.0 100.0 125.0 150.0 175.0 200.0 225.0

Tme0BCC
TEMP1: 30.0 C TIME1: 0.0 min RATE1: 10.0 C/min
TEMP2: 250.0 C

JFC
PERKIN-ELMER
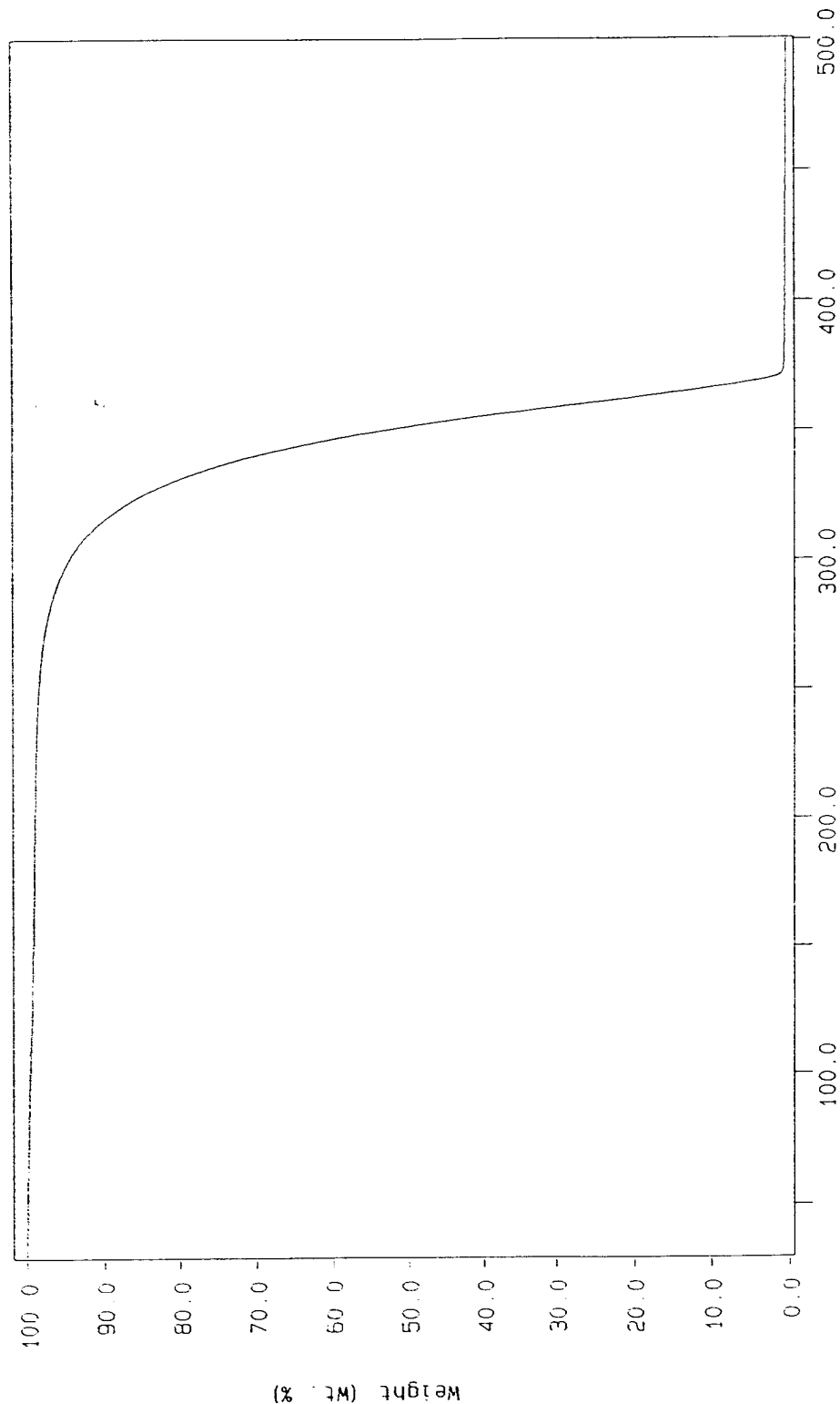7 Series Thermal Analysis System
Tue Jun 7 16:14:48 1994

Fig 10

Curve 1 TGA
File info. JLA16/4.1 Mon Jun 31 18:36:44 1994
Sample Weight: 2.539   mg

JFC1646/57A1

1 JFC1646/57A1
% Weight (Wt. %)

Temperature (°C)

Weight (Wt. %)

JFC1646/57A1

Weight (Wt. %)

TMeOBC

					RATE1:	10.0	C/min
TEMP1:	30.0	C	TIME1:	0.0	min	RATE2:	50.0	C/min
TEMP2:	400.0	C	TIME2:	0.0	min			
TEMP3:	900.0	C	TIME3:	5.0	min			

JFC
PERKIN-ELMER
7 Series Thermal Analysis System
Mon Jun 6 20:09:09 1994

Fig 11